A conserved mammalian mitochondrial isoform of acetyl-CoA carboxylase ACC1 provides the malonyl-CoA essential for mitochondrial biogenesis in tandem with ACSF3

Geoffray Monteuuis[a,1], Fumi Suomi[a,b,1], Juha M. Kerätär[a], Ali J. Masud[a] and Alexander J. Kastaniotis[a,2]

[a]Faculty of Biochemistry and Molecular Medicine, University of Oulu, FI-90014 Oulu, Finland;

[b]Current affiliation: Institute of Biotechnology, University of Helsinki, 00290 Helsinki, Finland.

[1]G.M. and F.S. contributed equally to this work

[2]To whom correspondence should be addressed. email: alexander.kastaniotis@oulu.fi; telephone number +358-294481196

Abstract

Mitochondrial fatty acid synthesis (mtFAS) is a highly conserved pathway essential for mitochondrial biogenesis. The mtFAS process is required for mitochondrial respiratory chain assembly and function, synthesis of the lipoic acid cofactor indispensable for the function of several mitochondrial enzyme complexes and essential for embryonic development in mice. Mutations in human mtFAS have been reported to lead to neurodegenerative disease. The source of malonyl-CoA for mtFAS in mammals has remained unclear. We report the identification of a conserved vertebrate mitochondrial isoform of ACC1 expressed from an ACACA transcript splicing variant. A specific knockdown of the corresponding transcript in mouse cells, or CRISPR/Cas9 mediated inactivation of the putative mitochondrial targeting sequence in human cells, lead to decreased lipoylation and mitochondrial fragmentation. Simultaneous knockdown of ACSF3, encoding a mitochondrial malonyl-CoA synthetase previously implicated in the mtFAS process, resulted in almost complete ablation of protein lipoylation, indicating that these enzymes have a redundant function in mtFAS. The discovery of a mitochondrial isoform of ACC1 required for lipoic acid synthesis has intriguing consequences for our understanding of mitochondrial disorders, metabolic regulation of mitochondrial biogenesis and cancer.

Keywords

ACC1 / acetyl-CoA carboxylase / mitochondrial Fatty acid synthesis / ACSF3/ malonyl-CoA / mitochondrial biogenesis

Introduction

Acetyl-CoA carboxylase (ACC) catalyzes the first committed step of the fatty acid synthesis (FAS) process, producing the malonyl-CoA extender for fatty acyl group elongation by addition of a carboxyl moiety from carbonate to acetyl-CoA (1). ACCs are highly conserved in organisms from archaea to higher eukaryotes (2). In contrast to their bacterial counterparts, the eukaryotic ACCs are multifunctional enzymes, harboring all necessary activities required for the carboxylation reaction on a single polypeptide (1). Mammalian ACCs have been reported to exist either as soluble cytosolic variants (ACC1 in humans, encoded by the *ACACA* gene) serving as producer of malonyl-CoA for cytosolic FAS, or anchored to the cytoplasmic side of the outer mitochondrial membrane (ACC2 encoded by *ACACB*), where ACC contributes to the regulation of mitochondrial β-oxidation by controlling the rate of acyl group transfer into mitochondria (3). Thus, malonyl-CoA fulfils several additional roles within cells apart from acting as FAS extender by serving as a master regulator in a wide array of physiological processes linked to lipid metabolism. These include control of mitochondrial acetyl-CoA generation from fatty acids, the ketogenic response of the liver during fasting, balancing cardiac fuel usage and adjusting energy source selection in skeletal muscle (4).

It has been firmly established that mitochondria host a highly conserved FAS pathway (mtFAS). MtFAS follows the bacterial type II FAS mode (5), where the acyl carrier protein (ACP)-dependent synthesis of fatty acids is carried out by a series of discrete polypeptides catalyzing the individual reactions (6). The requirement of a separate mtFAS pathway, conserved from yeast to higher eukaryotes including humans, indicates an essential role of this process in mitochondrial function.

In *Saccharomyces cerevisiae*, all mtFAS components are essential for respiration. A complete set of enzymes of this pathway required to produce straight chain fatty acids has been identified in yeast, and functional mammalian orthologues of nearly all of the yeast mtFAS proteins have been

described (6). Radioisotope labeling incorporation study in mammalian heart and plant have shown the major mtFAS product is octanoyl-ACP, providing the precursor for endogenous synthesis of the lipoic acid cofactor essential for the catalytic activities of several key mitochondrial oxidative decarboxylation enzyme complexes. In mammals, pyruvate dehydrogenase, α-ketoglutarate dehydrogenase, branched chain ketoacid dehydrogenase, α-ketoadipate dehydrogenase and the glycine cleavage system depend on lipoic acid for their function (7-9). The mtFAS pathway is capable of synthesizing fatty acids longer than eight carbons, and there is evidence for an important role for mtFAS products longer than C8 in mitochondrial biogenesis (10).

The first cases of a novel neurodegenerative human disorder (MEPAN, mitochondrial enoyl-CoA reductase protein associated neurodegeneration) caused by recessive mutations in the MECR (mitochondrial enoyl-CoA/ACP reductase) protein of mtFAS have been reported recently (11). Owing to the large number of components involved in the mtFAS process, the identification of more cases of disease caused by mtFAS dysfunction is to be expected.

One fundamental aspect for which mammalian mtFAS has been described to deviate from the yeast mtFAS pathway is the generation of malonyl-CoA. Both mammalian ACC variants have been reported to contribute to the malonyl-CoA production in the extramitochondrial space, but not in the mitochondrial matrix, where the *S. cerevisiae* mtFAS ACC encoded by the non-canonically translated *HFA1* gene is localized (12,13). It has been suggested that mitochondrial propionyl-CoA carboxylase may be capable of producing malonyl-CoA in this compartment in mammals by using the much less preferred acetyl-CoA as a substrate (14). An important contribution to solving the question on the origin of mitochondrial malonyl-CoA for mtFAS was provided by Witkowski and coworkers, who reported that the mitochondrial ACSF3 malonyl-CoA synthase found in animals could fulfill such a function (9). However, the extent of contribution of this protein to mtFAS is not clear, as a knockdown of *ACSF3* expression in human cultured cells did not yield in decreased protein lipoylation, which can be observed in studies on the effects of knockdown of other

mammalian mtFAS components (15,16) and in fibroblasts obtained from MEPAN patients (11). Therefore, an alternative source may be postulated for malonyl-CoA production in mammalian mitochondria.

Here, we demonstrate the existence of highly conserved mammalian mitochondria-specific ACC1 isoforms required for lipoic acid synthesis and maintenance of tubular mitochondrial morphology in mammalian cultured cells. Our data indicate that mitochondrially targeted ACC1 and ACSF3 act in concert to provide malonyl-CoA in mitochondria. These results add a final piece to the mtFAS puzzle and have intriguing consequences to our understanding of regulation of mitochondrial function and energy metabolism in health and disease.

Experimental

Bioinformatics. The mouse and human *ACACA/Acaca* sequence data were obtained from Emsembl (http://www.ensembl.org). Of the 23 annotated *ACACA* transcripts, only the four variants encoding full size ACC1 were analysed (Figure 1). The alignment of the transcript variants of the human ACACA was produced using the ClustalW program (http://www.ebi.ac.uk/Tools/msa/clustalw2/) (Figure 1A) (17). Seven transcripts of mouse *Acaca* are annotated in the Emsembl database. The information on the two transcripts encoding full size mouse Acc1 as well as an incomplete 5'RACE-generated transcript is shown in the table in Figure S1 B. A transcript encoding a full size mouse Acc1 with a predicted mitochondrial import sequence (Acaca-202; protein ENSMUSP0000048865; mitochondrial import probability 0.8676) had been previously present in ENSEMBL but is currently not available anymore. For both human and mouse ACACA/Acaca transcript variants, the mitochondrial localisation prediction for the encoded proteins was carried out using MitoProtII (19), TargetP (20) and iPSORT(21).

Plasmids, cell lines, culture media and growth conditions. The oligonucleotide sequences used for plasmid construction and analyses in our study will be made available on request. The pEGFP-

N1 vector (Invitrogen, Carlsbad, CA, USA), GenBank accession #U55762) was provided by Dr. Sakari Kellokumpu (University of Oulu, Oulu, Finland). A sequence containing the first 513 nucleotides of the ACC1 ORF encoded by transcript variant ACACA-001 (ENST00000616317.4) was synthesized by Genscript (Jiangning, Nanjing, Jiangsu Province, China). A PCR product containing the first 111 nucleotides of this ORF, encoding the 37 amino acid N-terminal extension of ACC1 isoform 1 predicted to constitute an MTS, flanked by HindIII and PstI sites, was cloned into vector pEGFP-N to generate an in-frame fusion of the N-terminal region of ACC1 harboring the putative MTS (MWWSTLMSILRARSFWKWISTQTVRIIRAVRAHFGGI) to EGFP. For the oligonucleotide design for mouse knockdown (KD) studies, the sequences of the two isoforms of *Acaca*/Acc1 from mouse are referred to (Acaca-001 and Acaca-005, Figure S1). Three KD cassettes targeted the homologous sequence shared by cytosolic and putative mitochondrial transcript variants (A1,A2, A3), while two other cassettes targeted the exon predicted to encode the mouse Acc1 isoform 1 MTS (M1,M2). Plasmids and methods used for the KD cassette generation have been described before (22). Briefly, for the shRNA knockdown of the ACC1 in mouse NIH3T3 cell lines, pRVH1-puro (23), pVSV- and pSUPER (24) were provided by Aki Manninen (Biocenter Oulu, University of Oulu, Oulu). Oligonucleotides encoding shRNAs were cloned into pSUPER according to reference (24). The shRNA expression cassette was then transferred into the XhoI/EcoRI site of the pRVH1-puro. Mouse 3T3 cell lines stably expressing *Acaca* KD cassettes were generated by retroviral transduction. The human Phoenix gag-pol packaging cell line (American Type Culture Collection with authorization by Garry Nolan, School of Medicine, Stanford University, Stanford CA) was provided to us by Aki Manninen (Biocenter Oulu, University of Oulu, Oulu, Finland). The construct used for knockdown of expression of the mouse mtFAS Mecr expression has been described (22). All cell lines were maintained at 5% CO2 at 37°C in Dulbecco's Modified Eagle Medium (DMEM, 4.5g/L glucose) (Invitrogen, Carlsbad, California, USA) supplemented with 10% fetal bovine serum (FBS) (HyClone, Cramlington, UK) and

GlutaMAX^{TM} (ThermoFisher Scientific, Waltham, MA, USA). For the investigation of functionality of the putative MTS constituted by N-terminal sequence of the human ACC1, the HEK293T cell line was used. For transfection, 150,000 cells were seeded in each well of a 6-well plate and incubated at 37°C. After 24 hours 1µg plasmid, 97µl Opti-MEM (Invitrogen, Carlsbad, California, USA) and 3µl FuGENE 6 (Roche Diagnostics, Indianapolis, IN, USA) were added. After 72 hours, the post-transfection, the cells were fixed with 4% para formaldehyde (PFA) for the slide preparation. VECTASHIELD HardSet Mounting Medium with DAPI (VECTOR, CA, USA) was used.

Generation of Acaca and Mecr shRNA Knockdowns. Acaca Knockdown - As a control, empty vector RVH1 was used for the transfection. The Acaca-005 sequence (ENSMUST00000133811.2) was used to design the KD cassettes targeted to the predicted MTS. This transcript variant is annotated as incomplete and was identified by 5' RACE (25). As the overall structure of the mouse *Acaca* gene would allow to produce a full size mouse Acc1 harbouring this N-terminal extension, we chose to target this sequence for our KD studies. In 2011, ENSEMBL annotated a transcript Acaca-202 which showed highly homologous sequence with Acaca-005 coding for a protein harbouring the MTS and of a total length of 2382 amino acids. This transcript is currently not available on the ENSEMBL database anymore. A detailed description of the knockdown procedure can be found in the supplementary Experimental section. After the selection for successfully infected cells, protein and RNA were isolated for analysis and real-time quantitative PCR.

***Mecr* Knockdown** –*Mecr* shRNA knockdown cell lines were generated using NIH3T3 cell line as described previously (22). Cell lines were maintained as above, supplemented with penicillin-streptomycin (SIGMA-Aldrich, Saint Louis, Missouri, USA).

Generation of the ACSF3 esiRNA KD. HEK293 cells were maintained in Dulbecco's modified Eagle's medium supplemented with 10% fetal bovine serum at 37 °C in a 5% CO_2 atmosphere. Mission esiRNA reagents, as well as control esiRNA (targeted against the GFP), were purchased from SIGMA-Aldrich (Saint Louis, Missouri, USA). Transfection was performed using *JetPrime (Polyplus, Illkirch-Graffenstaden, France) transfection kit.* HEK293T cells were seeded at a density of 2×10^4 cells per 450 ul in each well of 24 well plates. EsiRNA was diluted in 48µl Jetprime buffer, then 2µl of JetPrime reagent was added to the mixture and incubated at 20 °C for 15 min. The final mixture was added to culture plate wells, resulting in a final esiRNA concentration of 40 and 60 nM. Cells were collected after 72h incubation and protein and total RNA samples were prepared.

Generation of HEK293 ACACA MTS Knock out derived cell lines. CRISPR/Cas9-mediated genome editing was used to generate a HEK293 (Human embryonic kidney) derived cell with an inactivated the ACC1MTS (Figure S4A). We used a commercial, custom-manufactured CRISPR/Cas9 genome editing construct based on the pSpCas9(BB)-2 A-GFP vector containing a sgRNA expression construct (SIGMA-Aldrich, Saint Louis, Missouri, USA) designed to target the exon encoding the ACC1 MTS. The supplier used their own proprietary algorithms to choose a construct with maximum specificity. One single construct was proposed by SIGMA-Aldrich due to the short target area (ACACA exon 2/ENSE00003512420, 47 nucleotides: GTCTTTCTGGAAGTGGATATCTACTCAGACAGTAAGAATTATAAGAG).

HEK293T cells were transfected with this CRISPR/Cas9 genome editing construct. Cells expressing the CRISPR/Cas9 constructs were identified by fluorescence-activated cell sorting, and candidate clones for successful genome editing were identified by T7 endonuclease assay (See supplementary Experimental). PCR products of the edited region were cloned in a vector and several clones were subsequently sequenced to identify the mutations in the knockout cell line (Figure S4). Sequence alignments were generated using Clustal Omega (26).

Real time quantitative PCR. ***Acaca*** **shRNA KD** - Total RNA isolation (RNeasy Kit, QIAGEN, Hilden, Germany) and first-strand cDNA synthesis (RevertAid First Strand cDNA Synthesis Kit, Fermentas/Thermofisher Waltham, Massachusetts, USA) were done according to the manufacturers' protocols. 1µg of total RNA treated with DNase I was used for the reverse transcription reaction. 1/25 of the synthesized DNA was used for the 25µl PCR reaction. The Real Time PCR reaction was carried out using a TaqMan Gene Expression Assay (Invitrogen, Carlsbad, CA, USA) specific for the mouse Acaca (Mm01304277_m1) according to the manufacturer's protocol. As the internal control, the TaqMan Gene Expression Assay (Invitrogen, Carlsbad, CA, USA) specific for Eukaryotic 18s rRNA (4333960F) was used. In order to obtain a relative quantification, the ΔΔCt method was used in the analysis. Student's T-Test was employed as a parametric statistic tool for the analysis. The standard deviation was calculated to measure the amount of dispersion of the data set. **ACSF3 esiRNA KD**. Total RNA was isolated using the RNeasy Mini kit (Qiagen, Hilden, Germany) and treated with DNase (Qiagen, Hilden, Germany) to avoid genomic DNA contamination. Total RNA yield was determined using a Nano-drop® ND-1000 Spectrophotometer. Total RNA (150 ηg) was reverse transcribed using the RevertAid First Strand cDNA Synthesis Kit according to the manufacturer's instructions. The resulting cDNA was stored in aliquots at -70°C. Real-time PCR was performed with Taqman (Thermo SCIENTIFIC, Waltham, MA, USA) probes for human ACSF3 and as endogenous control Actin B was used. A 7500 Real-time PCR system (Applied Biosystems, Foster City, CA, USA) was employed for the Run and data analysis. Relative quantification and statistical analysis were carried out as described above.

Western blotting. ***Acaca*** **shRNA KD** - Protein extracts from the cells were prepared using the Proteojet Mammalian Cell Lysis Reagent (Thermo SCIENTIFIC, Waltham, MA, USA), according to the manufacturers' protocol. Mitochondria were extracted from the cell culture using the

Mitochondria Isolation Kit for Cultured Cells (Abcam, MA, USA) according to the manufacturer's protocol. The proteins were separated by SDS-polyacrylamide gel electrophoresis. The proteins were transferred to membrane nitrocellulose membrane (Bio-Rad TURBO 0.2 µm, Bio-Rad, Hercules, CA, USA) using the Trans-Blot Turbo (Bio-Rad, Hercules, CA, USA). The SIGMA-Aldrich (Saint Louis, MO, USA) Blocking Buffer was used for blocking of the membrane. Rabbit monoclonal acetyl-CoA carboxylase1 specific antibody (Millipore, Billerica, MA, USA) was used at a 1:1000 dilution. For rabbit polyclonal anti-lipoic acid antibody (Calbiochem, La Jolla, CA, USA) a 1:3000 dilution was used. The anti-β actin antibody (Novus Biologicals, Littleton, CO, USA) was used at a 1:5000 dilution. The secondary antibodies peroxidase conjugated goat anti-rabbit IgG (SIGMA-Aldrich, Saint Louis, MO, USA) and goat anti-mouse IgG (Bio-Rad, Hercules, CA, USA) were used at 1:10000 dilutions. Chemiluminescence detection was performed using the Immun-Star WesternC Kit (Bio-Rad, Hercules, CA, USA). The PageRuler ™ Prestained protein Ladder (Fermentas/Thermofisher Waltham, MA, USA) was used for the estimation of the relative molecular mass of proteins. The signal from the western blot was detected using the ChemiDoc XRS molecular imager (Bio-Rad, Hercules, CA, USA) and analysed with the Image Lab 3.0.1 software (Bio-Rad, Hercules, CA, USA) where applicable. The volume of the LA and actin signals was normalized using the global background subtraction method. **Mecr KD** - SDS-PAGE for the western blot using Mecr antibody was done using 12% Tris-glycine gel. SDS-PAGE for the western blot using lipoic acid antibody was done using 10% Tris-Glycine gel. Proteins on the gels were transferred on a nitrocellulose membrane using Trans-Blot Turbo system (Bio-Rad, Hercules, CA, USA). Membranes were blocked with Casein blocking buffer solution (SIGMA-Aldrich, Saint Louis, MI, USA). Membranes were probed using the following antibodies: For probing Mecr, as a primary antibody rabbit polyclonal anti-Mecr-IgG (Proteintech, Chicago, USA) and as a secondary antibody goat anti-rabbit-IgG-HRP conjugate (Hercules, California, USA). For probing lipoic acid, as a primary antibody rabbit anti-LA-IgG (Calbiochem, La Jolla, CA, USA) and as a secondary

goat anti-rabbit-IgG-HRP conjugate (Hercules, CA, USA). For probing Dlat, as a primary antibody mouse polyclonal anti-Dlat-IgG (Novus Biologicals, Littleton, Colorado, US), and as a secondary antibody goat anti-mouse-IgG-HRP conjugate (Madison, Wisconsin, USA). In all cases Porin (VDAC) was probed as a loading control using as a primary antibody mouse anti-Porin-IgG (Abcam, MA, USA) and as a secondary antibody goat anti-mouse-IgG-HRP conjugate. Signal was detected using Clarity ECL Western Blotting Substrate (Bio-Rad, Hercules, CA, USA) and the blots were imaged with Chemidoc XRS camera system (Bio-Rad, Hercules, CA, USA). **ACACA MTS KO –** Mitochondrial extracts (20µg) were loaded in a 10% SDS-PAGE gel (Bio-Rad, Hercules, Ca, USA), transferred to a nitrocellulose membrane (Bio-Rad, Hercules, California, USA) and blocked with 5% fat free dried milk powder dissolved in Tris-buffered saline containing 0,1 % Tween 20. After blocking, the membrane was incubated with the primary antibody, then washed in Tris-buffered saline containing 0.1% Tween 20 and incubated with the secondary antibody. A first screen to select potential knockout cell lines was done by using an anti-lipoic acid primary antibody (same Calbiochem monoclonal antibody as above, now sold by Merk Millipore, Billerica, Massachusetts, USA). Cell lines that lacked or displayed a reduced detectable signal for lipoylated proteins were subjected to a secondary immunoblot screen using antisera that recognize the DLST E2 subunit of α-ketoglutarate dehydrogenase (anti-Dihydrolipoamide S succinyltransferase E2, Mouse polyclonal) (Novus Biologicals, Littleton, CO, USA), or the DLAT protein (anti-Pyruvate Dehydrogenase E2, Mouse polyclonal, Novus Biologicals, Littleton, CA, USA). Goat anti-rabbit-HRP (1:10000, Abcam, MA, USA), anti-mouse-HRP (1:3333, Madison, WI, USA) were used as secondary antibodies. Clarity™ Western ECL Blotting Substrates (BioRad, Hercules, CA, USA) were used according to manufacturer's recommendations. Quantification of band intensities was performed using Image Lab software. To calculate the percent change of lipoylation in the ΔMTS-ACC1 mutant, three biological repeats (mitochondrial extract from separate cell cultivations) were analyzed. To obtain comparable results, ratios of the lipoylation signal over the corresponding β-

actin loading control were determined, and the thus normalized level of wild type lipoic acid over wild type β-actin defined as 100% for each individual experiment. Percent lipoic acid in the sample was determined as the fraction of [LA/β-actin] from the ΔMTS-ACC1 mutant compared to [LA/β-actin] of wild type cells. A two-tailed student's T-Test was used to determine the p-value.

Fluorescence microscopy. **Colocalization study** – HEK293 cells were seeded on a coverslip in a 12 well plate containing Dulbecco's Modified Eagle Medium (DMEM), high glucose complemented with 1mM Uridine, 5mM Sodium Pyruvate, 10% (v/v) fetal calf serum, 1x Essential Amino Acids, 1x Penicillin-Streptomycin at 37°C under an atmosphere of 5% CO_2 and 95% air. After the cells had attached, transfection was performed using FuGENE HD Transfection (Promega, Madison, WI, USA) according to the manufacturer's instructions. To detect the mitochondrial network, cells were also transfected with the MtDsRED plasmid (pDsRED-Mito, Clontech/Takara Bio, Mountain View, CA, USA). After 24h incubation, cells were fixed with 4% paraformaldehyde and fluorescence microscopy pictures were taken with Zeiss LSM700 confocal and 3D images were created from stacks processing analysis. The overlap coefficient (Manders) and correlation coefficient (Pearson) were collected from the 3D representation.

***Acaca* shRNA KD.** For the study of the mitochondrial morphology of mouse Acaca KD cell lines, a ZEISS (ZEISS, Oberkochen, Germany) Observer-Z1confocal microscope with a ZEISS LSM700 unit was used. The images were obtained with a plan APOCHROMAT 60 x objective oil lens using the ZEN 2009 software. The MitoTracker Red CMX Ros (Invitrogen, Carlsbad, CA, USA) was used to stain the mitochondria following the manufacturer's protocol. **Mecr KD** – Sub-confluent cell lines were seeded on glass coverslips on cell culture plates and grown overnight. MitoTracker Red CMXRos (Invitrogen, Carlsbad, CA, USA) diluted in DMEM at concentration of 100 nM was used to stain the mitochondria of the cells. Cells were fixed using 4% paraformaldehyde solution and the glass coverslip was mounted on microscopy slide using Vectashield Mounting Medium with DAPI (Vector Laboratories, Burlingame, CA, USA). Mitochondrial morphology was imaged

using Zeiss LSM 700 confocal microscope. **ACACA MTS KO** – HEK293 cells (WT and ACACA MTS KO) were seeded on a coverslip in a 6 well plate containing Dulbecco's Modified Eagle Medium (DMEM), high glucose complemented with 1mM Uridine, 5mM Sodium Pyruvate, 10% (v/v) fetal calf serum, 1x Essential Amino Acids, 1x Penicillin-Streptomycin at 37°C under an atmosphere of 5% CO_2 and 95% air. After the cells have attached, transfection was performed using FuGENE HD Transfection (Promega, Madison, WI, USA) according to the manufacturer's instructions. After 48h incubation, cells were fixed with 4% paraformaldehyde and fluorescence microscopy pictures were taken with a Zeiss LSM700 confocal microscope.

Results

The human ACACA-001 encoded ACC1 protein isoform harbors a functional N-terminal mitochondrial targeting signal (MTS).

An intramitochondrial mammalian acetyl-CoA carboxylase has not been described to date. Inspired by our previous finding that cytosolic and mitochondrial ACCs in yeast were originally dually localized but expressed from one gene (13), we investigated transcript variants of ACCs in the human genome listed in ENSEMBL (27). The database lists four transcript splicing variants encoding full size ACCs that vary at the predicted N-termini (Figure 1A). The probabilities of these N-terminal sequences serving as mitochondrial import signals were assessed using MitoProt II (19), TargetP (20) and iPSORT (21). Our results indicate that the ACC1 protein isoform 1 produced from the human transcript *ACACA-001,* is predicted to be mitochondrially localized with high probability by all three algorithms (Figure. 1B).

We generated a construct that expresses a fusion of the first amino acid 37 residues of ACC1 isoform 1 to GFP in HEK293 cells in order to investigate if this N-terminal sequence constitutes a functional MTS. Figure 1A depicts the ACC1 amino acid sequence fused to GFP in gray highlights. Fluorescence microscopy of cells expressing a control GFP construct without the predicted N-

terminal MTS exhibited diffuse green fluorescence and negative correlation with the MtDsrRED mitochondrial marker signal (Figure. 1C, E). In contrast, when GFP appended with the predicted MTS of ACC1 isoform 1 was expressed in these cells, the green fluorescent signal showed a significantly higher overlap and a positive correlation with the MtDsRED mitochondrial marker (Figure. 1D, E).

Mitochondrial targeting sequences of mammalian ACACAs are highly conserved.

To investigate how well the N-terminal MTS is conserved among species, we conducted a N-BLAST search against vertebrate protein sequences using the predicted MTS of the human ACC1 isoform 1 protein. Our search returned ACC1 proteins from a wide range of mammalian species. Investigation of the N-terminal sequences of these ACC1 orthologs using the MitoProtII, Target P and iPSORT program indicated that many of these candidate proteins were predicted to harbor sequences with high probability of constituting N-terminal MTSs. A list with selected homologs can be found in **(**Table 1), among them also a putative alligator sequence as an example of a non-mammalian vertebrate.

Several mRNA variants of *Acaca* are documented for mouse in the ENSEMBL database. *Acaca-005*, an incomplete transcript identified by 5' RACE, is predicted to encode a variant of Acc1 with an extended N-terminus compared to the *Acaca*-001- or *Acaca*-201 encoded full-size Acc1 (Figure S1A). Mitochondrial localization prediction analysis of the N-terminal extension with the three independent algorithms indicated a high probability of constituting an MTS with an MMP cleavage site at amino acid 28 (Figure S1A, cleaved sequence underlined), leaving the Acc1 enzyme intact after removal of the signal peptide. A predicted protein isoform containing this N-terminus and with high probability of mitochondrial localization is listed in Genbank as XP_006532016.1 (Table 1).

A specific knockdown of the putative mitochondrial isoforms of mouse Acaca results in mitochondrial defects.

A knockdown targeting total *Acaca* transcripts can be predicted to exert pleiotropic negative effects on the cellular metabolism, since Acc1 plays essential roles in many important processes. Hence, we designed constructs for retrovirus-mediated permanent knockdowns (23) expressing shRNAs specifically targeted for RNAi towards the section of these transcripts predicted to encode the putative MTS of Acc1. In addition, we generated constructs targeting all *Acaca* transcripts in mouse NIH 3T3 cells for comparison. Two KD constructs specific for the transcript encoding the putative mitochondrial isoform and three KD constructs targeting all full size mRNA species were tested. Only one of the former (referred to M1) and one of the latter (A1) resulted in the desired KD effect. Cells expressing either one of the effective shRNA constructs grew slower than the cells infected with a virus harboring the empty control construct, not expressing shRNA.

The transcript levels of *Acaca* in the total Acc1 KD cell lines (A1) was reduced to less than half of the level in controls, while cell lines knocked down specifically for the putative mitochondrial isoform of Acc1(M1) showed reduction of expression levels by about 15 % compared to the control (Figure S2). Congruently, western blotting confirmed that there was a clear reduction of Acc1 protein levels in the A1 KD cell line, while no clear decrease of Acc1 could be detected in the M1 knockdown cells (Figure 2A, upper panel).

The yeast mitochondrial Hfa1 ACC provides the malonyl-CoA extender unit to mtFAS, which produces the octanoic acid precursor of lipoic acid. To investigate if mtFAS is affected by the *Acaca* KDs in mouse cells, we analyzed lipoic acid contents of the *Acaca* KD cell lines. Western blots of protein extracts from KD and control cell lines were probed with anti - lipoic acid antibody. Initially, extracts analyzed from the slow growing M1 and A1 cell lines displayed a reduction or disappearance, respectively, of the lipoylation signal of a specific subpopulation of the lipoylated

Dlat subunit of the PDH complex (Figure S3 A). This phenotype was reminiscent of a Dlat lipoylation defect in mtFAS we observed upon knockdown of expression of mouse *Mecr*, encoding mitochondrial enoyl-CoA/ACP reductase of mtFAS (Figure S3B, left lower panel). Reduction of the lipoylated signal was accompanied by a concomitant reduction of total Dlat (Figure S3C). Later analysis, using a different lot of the lipoic acid antibody, did not reveal such a clear separation into two different subspecies, but confirmed an overall reduction of lipoylation in both A1 and M1 cell lines compared to the control (Figure 2A, lower panel).

We also investigated if inactivation of the mitochondrial ACC isoform would have consequences for the mitochondrial morphology in the KD cell lines. Compared to the control cell line, which displayed mostly tubular mitochondrial structure, knockdown of the mitochondrial isoform of Acc1 resulted in mitochondrial fragmentation, (Figure 2B, central panels). Like our lipoylation analysis results, these phenotypes correlate well with the data we obtained in *Mecr* KD studies (Figure S3).

CRISPR/Cas9 mediated inactivation of the predicted MTS of human ACC1 leads to lipoylation defects and altered mitochondrial morphology.

Our mouse bioinformatics data as well as the results of the *Acaca* KD experiments supported our hypothesis of the presence of mitochondrial isoforms of Acc1 in mammals. Due to the rather short target area of the extra exon of the mouse RNA encoding the putative mitochondrial Acc1 isoform, were unable to generate an shRNA construct that would have allowed us to independently verify an effect of a knockdown of this splicing variant on lipoylation in mouse. To strengthen our data, we set out to investigate if results similar to the data as obtained by experiments with mouse cultured cells could be independently obtained using a heterologous mammalian cell model system. As our studies on the functionality of the putative MTS harbored by isoform 1 of human ACC1 indicated that this protein variant is likely to localize to mitochondria, we decided to again turn to

human cells to address the question on a mitochondrial function of ACC1, employing CRISPR/Cas9 editing (29). We purchased a CRISPR/Cas9 editing construct designed by a commercial supplier (SIGMA-Aldrich) based on the bioinformatics and experimental evidence we had previously generated. Using this construct, we edited the genome of the HEK293 cell line to harbor mutations that were predicted to inactivate the putative MTS encoded by the *ACACA*-transcript isoform 1. The clones were initially screened with the T7 endonuclease I assay for successful editing, and the presence of inactivating mutations was confirmed by sequencing (Figure S4). As shown in the alignment of the alleles found in the ΔMTS-ACC1 clone to the WT sequence, we were able to obtain *ACACA* alleles edited to harbor indel mutations in the sequences encoding the predicted MTS of ACACA. We found a 1 bp insertion in one of the alleles and a 2 bp deletion in the other *ACACA* allele, in both cases leading to reading frame shifts and introduction of early stop codons (Figure S4B/C). The sequence encoding the part of ACC1 shared by all isoforms, representing the active enzyme, is predicted to remain intact in these alleles (Figure S4C**)**.

We first examined the level of ACC1 from total cell extracts by using anti ACC1 serum. Similar to our observations in the mouse M1 knockdown cell line describe above, we were unable to detect any obvious change of ACC1 levels in the ΔMTS-ACC1 compared to WT. In contrast, we were able to observe a robust decrease of the level of lipoylated DLAT, the pyruvate dehydrogenase E2 subunit to 35.9 (+/-28) percent (n=3, p 0.019) compared to wild type in crude mitochondrial extracts. Concomitantly, overall DLAT protein levels appeared reduced when we probed with an antibody specific for this E2 subunit of PDH (Figure 3A) similar to the result we obtained using the *Mecr* KD mouse cell line (Figure S3A). As in our analysis of the mouse Acc1 isoform 1 KD cells, we also investigated the effect of inactivation of the predicted MTS of human ACC1 on mitochondrial morphology. To visualize the mitochondria, WT and ΔMTS-ACC1 HEK293 cells were transfected with a plasmid that target the Green Fluorescence Protein to the outer membrane of the mitochondrial compartment. Our analysis of confocal microscopic image of the fluorescent

mitochondrial network in the ΔMTS-ACC1 cells indicated a severe fragmentation phenotype (Figure 3B).

ACC1 and ACSF3 operate in concert in protein lipoylation.

Complete inactivation of the ACC1 MTS in HEK293 cells only leads to partial loss of lipoylation in the ΔMTS-ACC1 cells. It has been suggested previously that ACSF3, a mitochondrial malonyl-CoA synthetase, is acting as the malonyl-CoA provider for mtFAS (9). Despite the appropriate location and function of this enzyme, however, an RNAi mediated knockdown of *ACSF3* in HEK293 cells line did not result in a protein lipoylation defect (9). To test the hypothesis that ACSF3 acts as a malonyl-CoA producer in a parallel fashion to ACC1, we investigated the effect of ACSF3 depletion on protein lipoylation in the ΔMTS-ACC1 cell line. Using 40 nM of ACSF3 siRNA, expression of ACSF3 was reduced to 60 % compared to the control after 72 hours (Figure S5**)**. Similar to the results obtained by Witkowski *et al* (30), this reduction of ACSF3 expression did not result in any detectable loss of lipoylation. However, when we treated the cells with 60 nM ACSF3 siRNA, reducing ACSF3 transcript levels to 40 % of WT expression, we were able to observe a mild hypolipoylation phenotype (Figure 3C). Moreover, when ΔMTS-ACC1 cells were exposed to ACSF3 siRNA at 40 nM concentration, we were not able to detect further reduction of DLAT lipoylation, while lipoyl-DLAT was reduced to barely detectable levels in ΔMTS-ACC1 cells treated with 60nM siRNA specific for ACSF3. These results are consistent with the model that ACSF3 and the mitochondrial isoform of ACC1 operate in tandem to supply malonyl-CoA to human mtFAS.

Discussion

The role of malonyl-CoA as regulator and coordinator of fatty acid metabolism has been long acknowledged. Apart from acting as the basic building blocks for FAS, the cytosolic concentration of malonyl-CoA is the cellular indicator of availability of acetyl-CoA in this compartment, which

controls the activity of mitochondrial carnitine palmitoyl transferase and therefore -by extension- the β-oxidation activity in mitochondria. We have previously suggested that mtFAS may act as an intramitochondrial acetyl-CoA sensor (10). Our work presented here provides evidence that mammalian ACC1 and ACSF3 collaborate in the production of malonyl-CoA required for mtFAS, indicating an important role of ACC1 in acetyl-CoA sensing also in mitochondria, with malonyl-CoA acting as a master signal of energy metabolism.

Our data provides clear evidence that the conserved N-terminal extension of ACC1 isoform 1 in humans acts as a functional mitochondrial targeting signal. Our further analysis demonstrates that a specific knockdown of the corresponding isoform in mouse results in lipoylation and mitochondrial morphology defects congruent with the phenotypes of a knockdown of the transcript of *Mecr* of mtFAS.

Furthermore, we show that inactivation of this sequence by genomic editing of the targeting-signal encoding sequence in human cells produces congruent results. All this evidence points to a role of ACC1 isoform 1 in mtFAS, and adds the last missing piece to the puzzle of mtFAS components in mammals. The reason why ACC1 had not been previously reported to be localized in mitochondria is likely due the phenomenon called “eclipsed distribution” (31), where the localization of a small sub-population of a protein is not readily detected because the overwhelming majority is found elsewhere in the cell. Such a case has been well documented for aconitase in yeast (31), although with reversed roles compared to mammalian ACC1. The bulk of aconitase, which has long been regarded as mitochondrial marker protein, is localized to mitochondria where it participates in the TCA cycle. However, a minute amount of this enzyme is present in the cytosol, where it serves in the glyoxylate cycle. There are a few examples of mitochondrial isoforms of proteins in mammals by alternative splicing-generated by addition of a sequence encoding an N-terminal MTS (32), but no systematic investigation has been made to address this question. While proteomics data do not currently support the notion that protein isoform generation by alternative

splicing is a major contributor to proteome complexity (33), it cannot be ruled out that low abundant alternative protein variants may escape grand scale analyses approaches.

In contrast to a previous report on the effects of a knockdown of expression of ACP in a human cell culture model, which presented data implying that the DLAT protein turns over independently from the lipoic acid (16), we observed a decrease of Dlat protein concomitantly with the decrease in lipoylation in both of our models systems. Feng et al., however, used a transient knockdown approach for their study. In contrast, our approaches produced a permanent knockdown mouse cell line and a human cell line that carries persisting genomic mutations in activating the MTS of ACC1. We therefore surmise that the disappearance of the Dlat/DLAT proteins in our studies are due to prolonged de-lipoylation of the protein, eventually leading to its disappearance.

It is worth noting that, like mammals, apparently also many fungi also produce both the cytosolic and the mitochondrial matrix versions of ACC from one gene (13). As an interesting twist in the fungal case, however, these lower eukaryotes seem to prefer generating the mitochondrial isoform by translation from a non-AUG initiation codon upstream from the canonical AUG that initiates production of the cytosolic form (13), rather than using a mechanism involving an alternative exon. This may be due to the fact that the extremely streamlined fungal genomes generally contain very few introns, and using alternative translation initiation mechanism is the most frugal approach to making alternate versions of proteins that are required in multiple location.

As an additional intriguing deviation in mammals from the yeast model, animal ACC1 apparently works in concert with a malonyl-CoA synthetase - ACSF3 - in the generation of malonyl-CoA. Why this apparently redundant function exists may remain subject of speculation. A fundamental difference between yeast and mammalian mitochondria is the lack of β-oxidation in mitochondria of the former. Due to the alternative source of acetyl-CoA directly produced in the mammalian organelle, an additional layer of control of mtFAS may be required.

In spite of this alternative source of malonyl-CoA produced by the ACSF3 enzyme, our data indicates that the general mechanism of malonyl-CoA generation for mtFAS is conserved from yeast to man. Poignantly, while monocotyledon plants have been shown to utilize ACCs in malonyl-CoA synthesis for mtFAS (34), dicots have recently been reported to employ a mitochondrial isoform of a malonyl-CoA synthetase named AEE13 for mtFAS/protein lipoylation (35).

ACC1 (*ACACA*) is listed in Mitocarta as a potential mitochondrial disease gene (36). As we provide evidence for a role of a mitochondrial isoform of ACC1 in mtFAS, mutant variants of ACC1 with compromised enzymatic function or dysfunction of the mitochondrial targeting signal, for example due to a splicing defect, may indeed lead to a mitochondrial disease phenotype. It should therefore be a matter of investigation if such deficiencies could be the contributing to neurodegenerative disease phenotypes similar to the recently described MECR dysfunction in MEPAN (11). Several cases of ACSF3 disorder have been reported, and patients display symptoms that partially overlap with the symptoms of MEPAN patients (37).

Presence of ACC1 in mitochondria also adds a new aspect to the proposed role of this enzyme in cancer. Presence of ACC1 is absolutely required for breast cancer cell survival (38) and translation of *ACACA* has been reported to be upregulated in breast cancer cells (39). In line with these observations, the inactive, phosphorylated form of ACC1 (P-ACC1) (40) has been shown to be associated with longer survival in lung cancer patients (41). A link of the proposed role of ACC1 in breast cancer exists via the BRCA1 oncogene, which has been reported to interact with P-ACC via its BRCT1 domains (42,43). The active phosphorylated form of BRCA1 is mainly localized to the nucleus and mitochondria (44), where ACC1 had not been found previously. As our data clearly suggests that also the ACC1 protein is present in this compartment, an interaction between BRCA1 and ACC1 in mitochondria may be a key component to the observed regulatory function of BRCA1 in energy metabolism (45). It has been shown that a low energy status can suppress the malignant

phenotype of certain cancers (46). Such a downregulation of energy metabolism may be achieved by attenuating mtFAS via maintaining an inactive form of mitochondrial ACC1 by BRCA1 binding, a regulatory mechanism that may be disturbed in cancer cells harboring BRCA1 mutations. Our work may therefore add a new facet to the proposed "Metabolic Syndrome of (Breast) cancer" (47).

Acknowledgements

We thank Prof. Kalervo Hiltunen for support, advice and critical reading of the manuscript, Dr. Aki Manninen for the help with the retrovirus mediated knockdown procedure, Hamayun Khan for his contribution in the setup of the initial mouse cell knockdown experiments, and Leila Polus for technical support. This work was supported by the Academy of Finland, the Sigrid Juselius Foundation, the Biocenter Oulu and AFM-Téléthon.

Conflict of interest

The authors declare that they have no conflict of interest.

Author contributions

AK conceived the study; GM, FS, JK and AJM performed in vitro and in vivo experiments; GM, FS, JK and AK did data analysis and wrote the manuscript.

References

(1) Tong L, Harwood HJ,Jr. Acetyl-coenzyme A carboxylases: versatile targets for drug discovery. J Cell Biochem 2006 Dec 15;99(6):1476-1488.

(2) Barber MC, Price NT, Travers MT. Structure and regulation of acetyl-CoA carboxylase genes of metazoa. Biochim Biophys Acta 2005 Mar 21;1733(1):1-28.

(3) Abu-Elheiga L, Brinkley WR, Zhong L, Chirala SS, Woldegiorgis G, Wakil SJ. The subcellular localization of acetyl-CoA carboxylase 2. Proc Natl Acad Sci U S A 2000 Feb 15;97(4):1444-1449.

(4) Saggerson D. Malonyl-CoA, a key signaling molecule in mammalian cells. Annu Rev Nutr 2008;28:253-272.

(5) White SW, Zheng J, Zhang YM, Rock. The structural biology of type II fatty acid biosynthesis. Annu Rev Biochem 2005;74:791-831.

(6) Kastaniotis AJ, Autio KJ, Keratar JM, Monteuuis G, Makela AM, Nair RR, et al. Mitochondrial fatty acid synthesis, fatty acids and mitochondrial physiology. Biochim Biophys Acta 2017 Jan;1862(1):39-48.

(7) Mayr JA, Feichtinger RG, Tort F, Ribes A, Sperl W. Lipoic acid biosynthesis defects. J Inherit Metab Dis 2014 Jul;37(4):553-563.

(8) Wada H, Shintani D, Ohlrogge J. Why do mitochondria synthesize fatty acids? Evidence for involvement in lipoic acid production. Proc Natl Acad Sci U S A 1997 Feb 18;94(4):1591-1596.

(9) Witkowski A, Joshi AK, Smith S. Coupling of the de novo fatty acid biosynthesis and lipoylation pathways in mammalian mitochondria. J Biol Chem 2007 May 11;282(19):14178-14185.

(10) Kursu VA, Pietikainen LP, Fontanesi F, Aaltonen MJ, Suomi F, Raghavan Nair R, et al. Defects in mitochondrial fatty acid synthesis result in failure of multiple aspects of mitochondrial biogenesis in Saccharomyces cerevisiae. Mol Microbiol 2013 Nov;90(4):824-840.

(11) Heimer G, Keratar JM, Riley LG, Balasubramaniam S, Eyal E, Pietikainen LP, et al. MECR Mutations Cause Childhood-Onset Dystonia and Optic Atrophy, a Mitochondrial Fatty Acid Synthesis Disorder. Am J Hum Genet 2016 Dec 1;99(6):1229-1244.

(12) Hoja U, Marthol S, Hofmann J, Stegner S, Schulz R, Meier S, et al. HFA1 encoding an organelle-specific acetyl-CoA carboxylase controls mitochondrial fatty acid synthesis in Saccharomyces cerevisiae. J Biol Chem 2004 May 21;279(21):21779-21786.

(13) Suomi F, Menger KE, Monteuuis G, Naumann U, Kursu VA, Shvetsova A, et al. Expression and evolution of the non-canonically translated yeast mitochondrial acetyl-CoA carboxylase Hfa1p. PLoS One 2014 Dec 11;9(12):e114738.

(14) Halenz DR, Feng JY, Hegre CS, LaneE MD. Some enzymic properties of mitochondrial propionyl carboxylase. J Biol Chem 1962 Jul;237:2140-2147.

(15) Chen C, Han X, Zou X, Li Y, Yang L, Cao K, et al. 4-methylene-2-octyl-5-oxotetrahydrofuran-3-carboxylic acid (C75), an inhibitor of fatty-acid synthase, suppresses the mitochondrial fatty acid synthesis pathway and impairs mitochondrial function. J Biol Chem 2014 Jun 13;289(24):17184-17194.

(16) Feng D, Witkowski A, Smith S. Down-regulation of mitochondrial acyl carrier protein in mammalian cells compromises protein lipoylation and respiratory complex I and results in cell death. J Biol Chem 2009 Apr 24;284(17):11436-11445.

(17) Li W, Cowley A, Uludag M, Gur T, McWilliam H, Squizzato S, et al. The EMBL-EBI bioinformatics web and programmatic tools framework. Nucleic Acids Res 2015 Jul 1;43(W1):W580-4.

(18) Claros MG, Vincens P. Computational method to predict mitochondrially imported proteins and their targeting sequences. Eur J Biochem 1996 Nov 1;241(3):779-786.

(19) Claros MG, Vincens P. Computational method to predict mitochondrially imported proteins and their targeting sequences. Eur J Biochem 1996 Nov 1;241(3):779-786.

(20) Emanuelsson O, Nielsen H, Brunak S, von Heijne G. Predicting subcellular localization of proteins based on their N-terminal amino acid sequence. J Mol Biol 2000 Jul 21;300(4):1005-1016.

(21) Bannai H, Tamada Y, Maruyama O, Nakai K, Miyano S. Extensive feature detection of N-terminal protein sorting signals. Bioinformatics 2002 Feb;18(2):298-305.

(22) Nair RR, Keratar JM, Autio KJ, Masud AJ, Finnila MA, Autio-Harmainen HI, et al. Genetic modifications of Mecr reveal a role for mitochondrial 2-enoyl-CoA/ACP reductase in placental development in mice. Hum Mol Genet 2017 Mar 24.

(23) Schuck S, Manninen A, Honsho M, Fullekrug J, Simons K. Generation of single and double knockdowns in polarized epithelial cells by retrovirus-mediated RNA interference. Proc Natl Acad Sci U S A 2004 Apr 6;101(14):4912-4917.

(24) Brummelkamp TR, Bernards R, Agami R. A system for stable expression of short interfering RNAs in mammalian cells. Science 2002 Apr 19;296(5567):550-553.

(25) Travers MT, Cambot M, Kennedy HT, Lenoir GM, Barber MC, Joulin V. Asymmetric expression of transcripts derived from the shared promoter between the divergently oriented ACACA and TADA2L genes. Genomics 2005 Jan;85(1):71-84.

(26) Goujon M, McWilliam H, Li W, Valentin F, Squizzato S, Paern J, et al. A new bioinformatics analysis tools framework at EMBL-EBI. Nucleic Acids Res 2010 Jul;38(Web Server issue):W695-9.

(27) Aken BL, Ayling S, Barrell D, Clarke L, Curwen V, Fairley S, et al. The Ensembl gene annotation system. Database (Oxford) 2016 Jun 23;2016:10.1093/database/baw093. Print 2016.

(28) Claros MG. MitoProt, a Macintosh application for studying mitochondrial proteins. Comput Appl Biosci 1995 Aug;11(4):441-447.

(29) Ran FA, Hsu PD, Wright J, Agarwala V, Scott DA, Zhang F. Genome engineering using the CRISPR-Cas9 system. Nat Protoc 2013 Nov;8(11):2281-2308.

(30) Witkowski A, Thweatt J, Smith S. Mammalian ACSF3 protein is a malonyl-CoA synthetase that supplies the chain extender units for mitochondrial fatty acid synthesis. J Biol Chem 2011 Sep 30;286(39):33729-33736.

(31) Regev-Rudzki N, Karniely S, Ben-Haim NN, Pines O. Yeast aconitase in two locations and two metabolic pathways: seeing small amounts is believing. Mol Biol Cell 2005 Sep;16(9):4163-4171.

(32) Pereira KD, Tamborlin L, Meneguello L, de Proenca AR, Almeida IC, Lourenco RF, et al. Alternative Start Codon Connects eIF5A to Mitochondria. J Cell Physiol 2016 Dec;231(12):2682-2689.

(33) Tress ML, Abascal F, Valencia A. Alternative Splicing May Not Be the Key to Proteome Complexity. Trends Biochem Sci 2017 Feb;42(2):98-110.

(34) Focke M, Gieringer E, Schwan S, Jansch L, Binder S, Braun HP. Fatty acid biosynthesis in mitochondria of grasses: malonyl-coenzyme A is generated by a mitochondrial-localized acetyl-coenzyme A carboxylase. Plant Physiol 2003 Oct;133(2):875-884.

(35) Guan X, Nikolau BJ. AAE13 encodes a dual-localized malonyl-CoA synthetase that is crucial for mitochondrial fatty acid biosynthesis. Plant J 2016 Mar;85(5):581-593.

(36) Calvo SE, Clauser KR, Mootha VK. MitoCarta2.0: an updated inventory of mammalian mitochondrial proteins. Nucleic Acids Res 2016 Jan 4;44(D1):D1251-7.

(37) Sloan JL, Johnston JJ, Manoli I, Chandler RJ, Krause C, Carrillo-Carrasco N, et al. Exome sequencing identifies ACSF3 as a cause of combined malonic and methylmalonic aciduria. Nat Genet 2011 Aug 14;43(9):883-886.

(38) Chajes V, Cambot M, Moreau K, Lenoir GM, Joulin V. Acetyl-CoA carboxylase alpha is essential to breast cancer cell survival. Cancer Res 2006 May 15;66(10):5287-5294.

(39) Yoon S, Lee MY, Park SW, Moon JS, Koh YK, Ahn YH, et al. Up-regulation of acetyl-CoA carboxylase alpha and fatty acid synthase by human epidermal growth factor receptor 2 at the translational level in breast cancer cells. J Biol Chem 2007 Sep 7;282(36):26122-26131.

(40) Kudo N, Barr AJ, Barr RL, Desai S, Lopaschuk GD. High rates of fatty acid oxidation during reperfusion of ischemic hearts are associated with a decrease in malonyl-CoA levels due to an increase in 5'-AMP-activated protein kinase inhibition of acetyl-CoA carboxylase. J Biol Chem 1995 Jul 21;270(29):17513-17520.

(41) Conde E, Suarez-Gauthier A, Garcia-Garcia E, Lopez-Rios F, Lopez-Encuentra A, Garcia-Lujan R, et al. Specific pattern of LKB1 and phospho-acetyl-CoA carboxylase protein immunostaining in human normal tissues and lung carcinomas. Hum Pathol 2007 Sep;38(9):1351-1360.

(42) Magnard C, Bachelier R, Vincent A, Jaquinod M, Kieffer S, Lenoir GM, et al. BRCA1 interacts with acetyl-CoA carboxylase through its tandem of BRCT domains. Oncogene 2002 Oct 3;21(44):6729-6739.

(43) Ray H, Moreau K, Dizin E, Callebaut I, Venezia ND. ACCA phosphopeptide recognition by the BRCT repeats of BRCA1. J Mol Biol 2006 Jun 16;359(4):973-982.

(44) Coene ED, Hollinshead MS, Waeytens AA, Schelfhout VR, Eechaute WP, Shaw MK, et al. Phosphorylated BRCA1 is predominantly located in the nucleus and mitochondria. Mol Biol Cell 2005 Feb;16(2):997-1010.

(45) Jackson KC, Gidlund EK, Norrbom J, Valencia AP, Thomson DM, Schuh RA, et al. BRCA1 is a novel regulator of metabolic function in skeletal muscle. J Lipid Res 2014 Apr;55(4):668-680.

(46) Swinnen JV, Beckers A, Brusselmans K, Organe S, Segers J, Timmermans L, et al. Mimicry of a cellular low energy status blocks tumor cell anabolism and suppresses the malignant phenotype. Cancer Res 2005 Mar 15;65(6):2441-2448.

(47) Brunet J, Vazquez-Martin A, Colomer R, Grana-Suarez B, Martin-Castillo B, Menendez JA. BRCA1 and acetyl-CoA carboxylase: the metabolic syndrome of breast cancer. Mol Carcinog 2008 Feb;47(2):157-163.

Species		Definition	GenBank accession no.	Mitoprot (CS)	TargetP (CS)	iPSORT Mitochondrial Prediction
Homo sapiens	Human	acetyl-CoA carboxylase 1 isoform 1	NP_942131.1	**0.9930 (13)**	**0.868 (22)**	YES
Mus musculus	Mouse	acetyl-Coenzyme A carboxylase alpha, partial	CAF02251.1	**0.1062 (NP)**	**0.075 (NP)**	NO
Mus musculus	Mouse	PREDICTED: acetyl-CoA carboxylase 1 isoform X2	XP_006532016.1	**0.7977 (28)**	**0.873 (19)**	YES
Macaca mulatta	Rhesus monkey	acetyl-CoA carboxylase 1 precursor	NP_001253707.1	**0.9855 (27)**	**0.815 (12)**	YES
Bos taurus	Cattle	acetyl-CoA-carboxylase alpha, partial	CAX51837.1	**0.9828 (13)**	**0.715 (12)**	YES
Ovis aries	Sheep	acetyl-CoA carboxylase-alpha	CAD92090.1	**0.9849 (35)**	**0.783 (34)**	YES
Pan troglodytes	Chimpanzee	PREDICTED: acetyl-coenzyme A carboxylase alpha	XP_511428.4	**0.9922 (13)**	**0.884 (22)**	YES
Oryctolagus cuniculus	Rabbit	PREDICTED: acetyl-CoA carboxylase 1 isoform X3	XP_008269381.1	**0.9817 (27)**	**0.820 (12)**	YES
Ailuropoda melanoleuca	Giant panda	PREDICTED: acetyl-CoA carboxylase 1 isoform X1	XP_019661138.1	**0.9846 (27)**	**0.831 (12)**	YES
Alligator mississippiensis	Alligator	PREDICTED: acetyl-CoA carboxylase 1 isoform X5	XP_014463555.2	**0.9275 (43)**	**0.930 (16)**	YES

Table 1. **Conservation of putative mitochondrial ACC isoforms in vertebrates.** The predicted MTS of the human ACC1 isoform 1 protein was used in an N-BLAST search against vertebrate protein sequences. The table lists of ten selected homologs predicted to localize to mitochondria with high probability. Mitochondrial localization prediction was carried out with MitoprotII, Target P and iPSORT mitochondrial import prediction software. Where the programs predicted a targeting sequence cleavage site, we have included this information (number of amino acids from initiation methionine) in brackets.

A

```
ACACA-001       MWWSTLMSILRARSFWKWISTQTVRIIRAVRAHFGGIMDEPSPLAQPLELNQHSRFIIGS 60
ACACA-009       -----------------------------------MDEPSPLAQPLELNQHSRFIIGS 23
ACACA-003       ------------------------------------------------------------
ACACA-002       ----------------------------------------------------MEG 3

ACACA-001       VSEDNSEDEISNLVKLDLLEEKEGSLSPASVGSDTLSDLGISSLQDGLALHIRSSMSGLH 120
ACACA-009       VSEDNSEDEISNLVKLDLLEEKEGSLSPASVGSDTLSDLGISSLQDGLALHIRSSMSGLH 83
ACACA-003       ------------------------------------------------MSGLH 5
ACACA-002       SPEENKEMRYYMLQ--------------------------------------RSSMSGLH 25
                                                                     *****

ACACA-001       LVKQGRDRKKIDSQRDFTVASPAEFVTRFGGNKVIEKVLIANNGIAAVKCMRSIRRWSYE 180
ACACA-009       LVKQGRDRKKIDSQRDFTVASPAEFVTRFGGNKVIEKVLIANNGIAAVKCMRSIRRWSYE 143
ACACA-003       LVKQGRDRKKIDSQRDFTVASPAEFVTRFGGNKVIEKVLIANNGIAAVKCMRSIRRWSYE 65
ACACA-002       LVKQGRDRKKIDSQRDFTVASPAEFVTRFGGNKVIEKVLIANNGIAAVKCMRSIRRWSYE 85
                ************************************************************
```

B

Name	Transcript ID	Length (aa)	Mitoprot (CS)	TargetP (CS)	iPSORT Mitochondrial Prediction
ACACA-001	ENST00000616317.4	**2383**	**0.993 (13)**	**0.868 (22)**	**YES**
ACACA-009	ENST00000614428.4	2346	0.0707 (NP)	0.070 (NP)	NO
ACACA-003	ENST00000617649.4	2268	0.0253 (NP)	0.403 (NP)	NO
ACACA-002	ENST00000612895.4	2288	0.0203(NP)	0.075 (NP)	NO

C

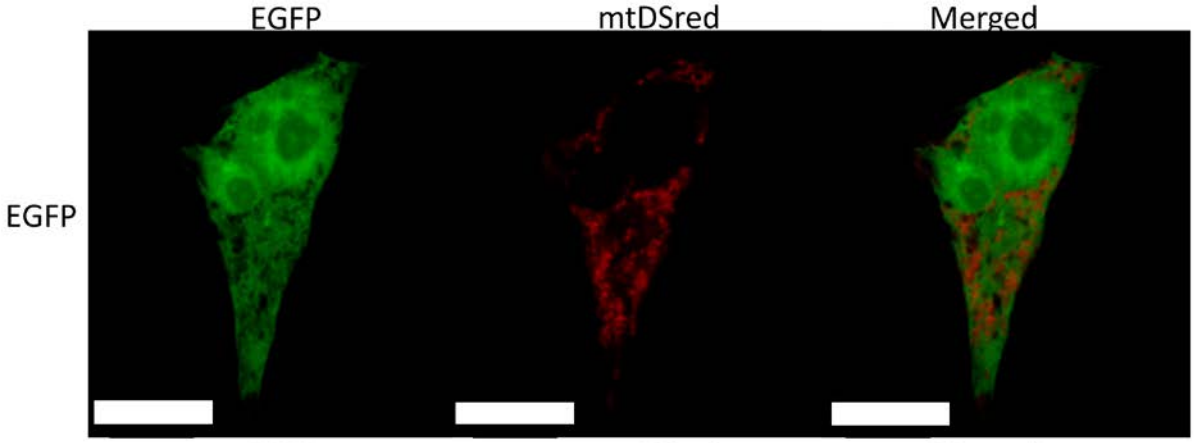

D

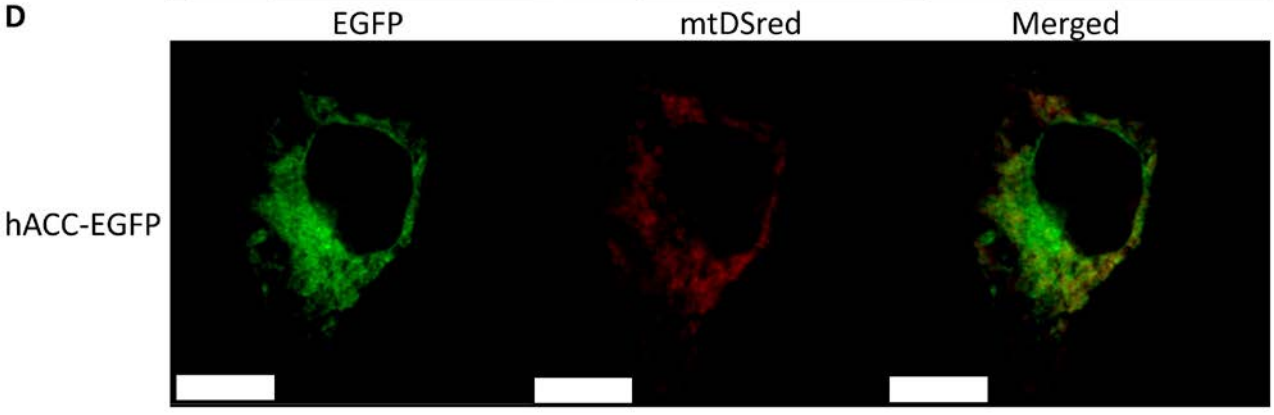

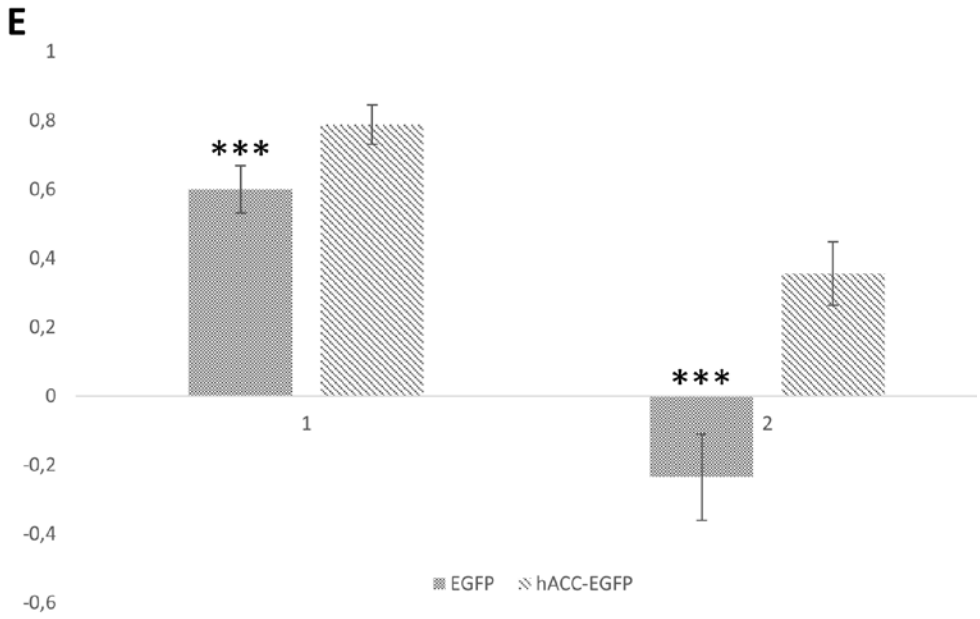

Figure 1. **The N-terminal extension of human ACC1 isoform 1 constitutes a mitochondrial targeting signal (MTS)**. **A)** Alignment of the predicted protein products of *ACACA* transcripts encoding full-size human ACC1. The N-terminal extension is marked by grey shading, the predicted MTS up to the signal peptide cleavage site is shown underlined and in bold letters. **B)** Transcript IDs, length of predicted proteins and MitoprotII, TargetP and iPSORT for mitochondrial import predictions for the polypeptides. NP: not predicted. **C)** and **D)** Fluorescence microscopy analysis of HEK293 cells expressing EGFP (**C**) or EGFP N-terminally appended with the N-terminal extension of human ACC1 isoform 1 shown in gray background in Figure 1A (**D**). To visualize the mitochondrial network, cells were co-transfected with the MtDsRED plasmid (red fluorescence panel). The fluorescence of EGFP lacking the N-terminal extension shows no correlation with the MtDsRED signal (**C**), while the N-terminally appended variant co-localizes with the mitochondrial stain (**D**). Scale bars are 10 µm. (**E**) Analysis of overlap (Manders coefficient, (1)) and correlation (Pearson coefficient (2)) of the MtDsRED signal with control EGFP versus hACC1-EGFP fluorescence. The hACC-EGFP signal shows higher overlap with the red fluorescence than the control construct and high positive correlation, while the EGFP control is negatively correlated with the mitochondrial fluorescence of the MtDsRED construct. Data were

collected from the 3D representation that were created from eight individual cells. Student T-test was performed. Errors bar indicate standard deviation (Manders *P* value: 0.0006 ; Pearson *P* value: 0.0001 **(E).**

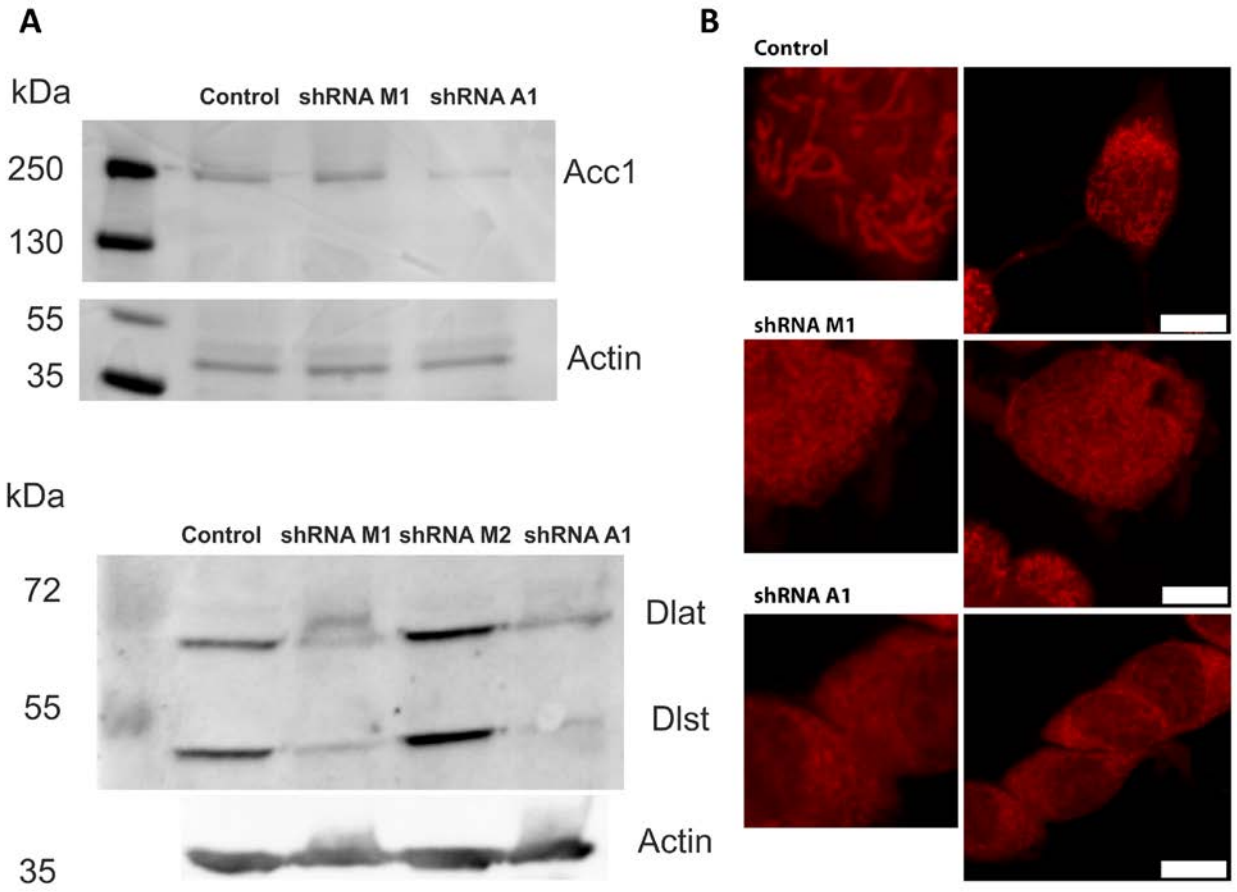

Figure 2. **The *Acaca* knockdown in mouse cells affects protein lipoylation and mitochondrial morphology**. **A)** Western blotting analysis of total cell extract from mouse NIH3T3 knockdown cell lines. The shRNAi targeting of total *Acc1* transcript (shRNA A1) but not the specific targeting of the transcript variant encoding the putative mitochondrial Acc1 isoform resulted in reduction of Acc1 protein levels in whole cell extracts (upper panel: anti-Acc1; loading control:β-actin). Protein lipoylation of the Dlat E2 subunit of pyruvate dehydrogenase as well as Dlst of α-ketoglutarate dehydrogenase was reduced in the *Acaca* KD targeting either the transcript variant encoding

cytosolic Acc1 or exclusively the variant encoding the mitochondrial isoform (lower panel, anti-lipoic acid; loading control:β-actin). The M2 lane between the M1 and A1 samples corresponds to the unsuccessful M2 knockdown cell line (see Results section and Figure S1) for which the analysis of the cell extract displayed a lipoylation pattern identical to the wild type sample. Dlat: dihydrolipoamide S-acetyltransferase, E2 component of the pyruvate dehydrogenase complex; Dlst: Dihydrolipoamide S succinyltransferase, E2 component of 2 oxoglutarate complex. Control: cells infected with virus carrying the the empty vector. **B)** Mitochondrial fragmentation upon knockdown of *Acaca* in mouse NIH3T3 KD cells. The control cells exhibit mostly reticular mitochondria, while the mitochondrial isoform-specific knowdown cells (shRNA M1) contain mostly fragmented mitochondria. Cells expressing the total *Acaca* knockdown shRNA (shRNA A1) have an intermediate mitochondrial morphology phenotype. Mitochondria are visualized with MitoTracker Red CMX Ros. Left panels are enlarged sections of the panels on the right. KD constructs used for the study are indicated on top of the left side panels. Cells were imaged using confocal microscopy. Scale bars are 10 μm.

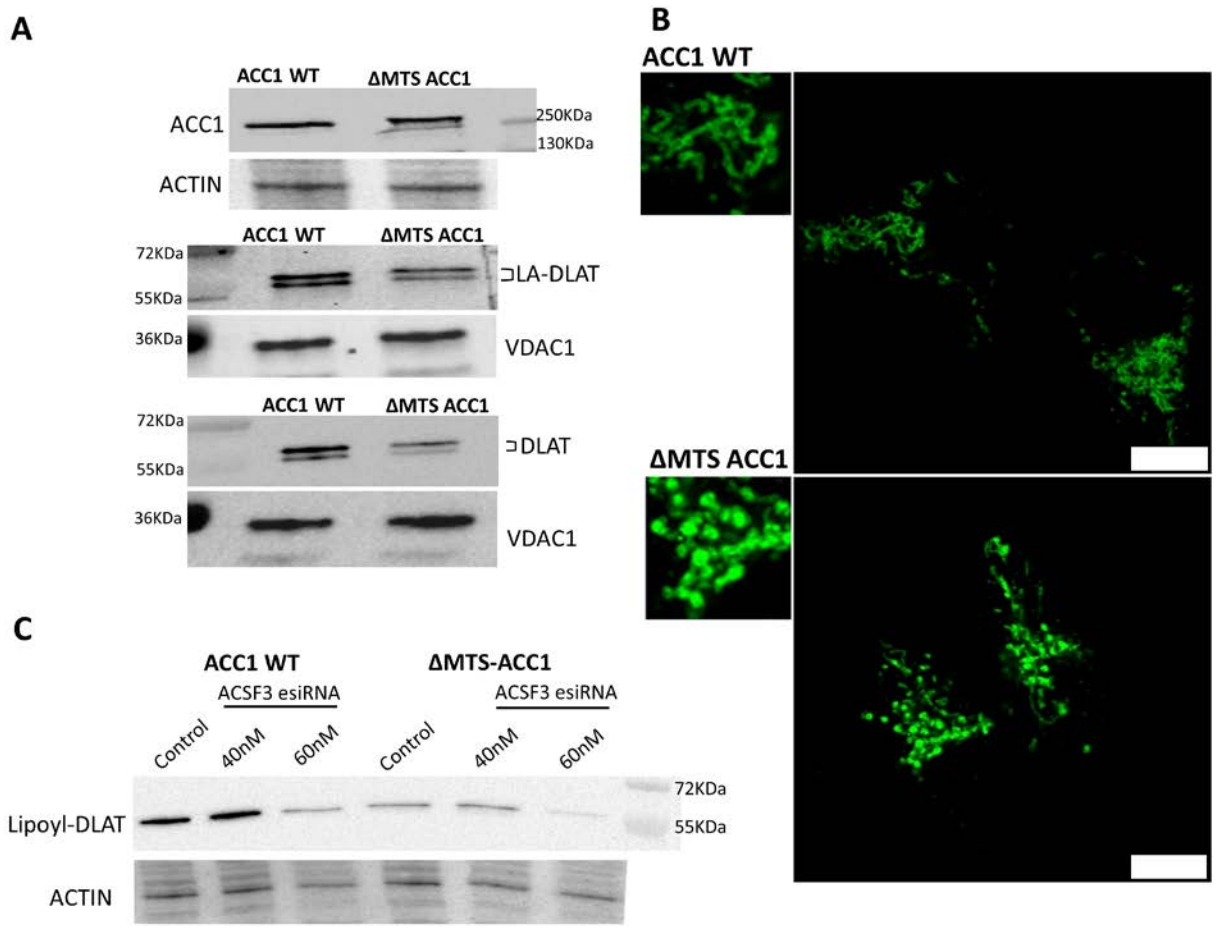

Figure 3. **Effect of CRISPR/Cas9-mediated inactivation of the ACC1 MTS in human cells on protein lipoylation and mitochondrial fragmentation and lipoylation defect by ACSF3 KD**. **A)** Protein lipoylation of the DLAT subunit was reduced in the ΔMTS-ACC1 cell line. Protein analysis by western blotting of HEK293 total cell extracts for the detection with anti-ACC1 (upper panel), with a corresponding loading control probing for β-actin. Analysis of mitochondrial extracts with anti-LA (Lipoic acid, middle panel) or anti-DLAT (dihydrolipoamide S-acetyltransferase, component E2 of the multi-enzyme PDH complex, lower panel) antiserum revealed a reduction of both lipoylation as well as DLAT protein. Anti-VDAC1 (Voltage-dependent anion-selective channel 1, antibodies were used as a loading control. **B)** Fragmentation of mitochondria in the ΔMTS-ACC1 human cell line. Cells were transfected with a plasmid expressing and targeting the GFP (Green fluorescent Protein) to the mitochondrial outer membrane. On the top panel, fluorescence microscopy picture of the HEK293 wild type control cells exhibiting reticular

mitochondrial structure, while ΔMTS-ACC1 cells depicted on the lower panels show mitochondrial fragmentation. Zoomed pictures are shown on the left panels. Cells were imaged using confocal microscopy. Scale bars are 10 µm. **C)** The DLAT subunit protein lipoylation defect was exacerbated by the ACSF3 KD in the ΔMTS-ACC1 cell line. Protein analysis by western blotting of the HEK293 cell extracts was carried out with anti-LA (Lipoic acid, upper panel) antibody. Anti-ACTIN (lower panel) antibody was used as a loading control.

Supplementary Figures

A

```
Acaca-001       ------------------------------------MDEPSPLAKTLELNQHSRFIIG 22
Acaca-201       ------------------------------------MDEPSPLAKTLELNQHSRFIIG 22
Acaca-005       MMWWSTLMSLLRASSFWRRISAETIRIIRALRAYFERIMDEPSPLAKTLELNQHSRFIIG 60
                                                    **********************

Acaca-001       SVSEDNSEDEISNLVKLDLEEKEGSLSPASVSSDTLSDLGISGLQDGLAFHMRSSMSGLH 82
Acaca-201       SVSEDNSEDEISNLVKLDLEEKEGSLSPASVSSDTLSDLGISGLQDGLAFHMRSSMSGLH 82
Acaca-005       SVSEDNSEDEISNLVKLDLEEKEGSLSPASVSSDTLSDLGISGLQDGLAFHMRSSMSGLH 120
                ************************************************************
```

B

Name	Transcript ID	Length (aa)	Mitoprot (CS)	Target P (CS)	iPSORT Mitochondrial Prediction
Acaca-001	ENSMUST00000103201.7	2345	0.36 (NP)	0.08 (NP)	NO
Acaca-201	ENSMUST00000020843.12	2345	0.10 (NP)	0.08 (NP)	NO
Acaca-005	ENSMUST00000133811.2	157*	**0.92 (28)**	**0.87 (19)**	**YES**

Figure S1. **Alignment of the N-terminal sequence encoded by mouse Acaca transcript variants reveal the presence of an N-terminal extension of the Acaca-005 encoded isoform constituting a mitochondrial import signal. A**) The amino acid sequence alignment shows that the predicted protein encoded by mouse Acaca-005 is N-terminally extended (underlined letters) compared to Acaca-001 or Acaca-201- encoded Acc1 variants. **B**) Transcript IDs, length of predicted proteins and MitoprotII, TargetP and iPSORT mitochondrial import prediction software for the different mouse Acc1 isoforms. Where available, cleavage site prediction (CS) is listed in brackets. *The Acaca-005 transcript listed in ENSEMBL is the results of 5'RACE analysis and therefore marked as incomplete. A full size protein containing the N-terminal sequence encoded by the Acaca transcript is listed in Genbank as XP_006532016.1. (see also Figure 2). A corresponding transcript named Acaca-202 was listed in ENSEMBLE previously but has since disappeared.

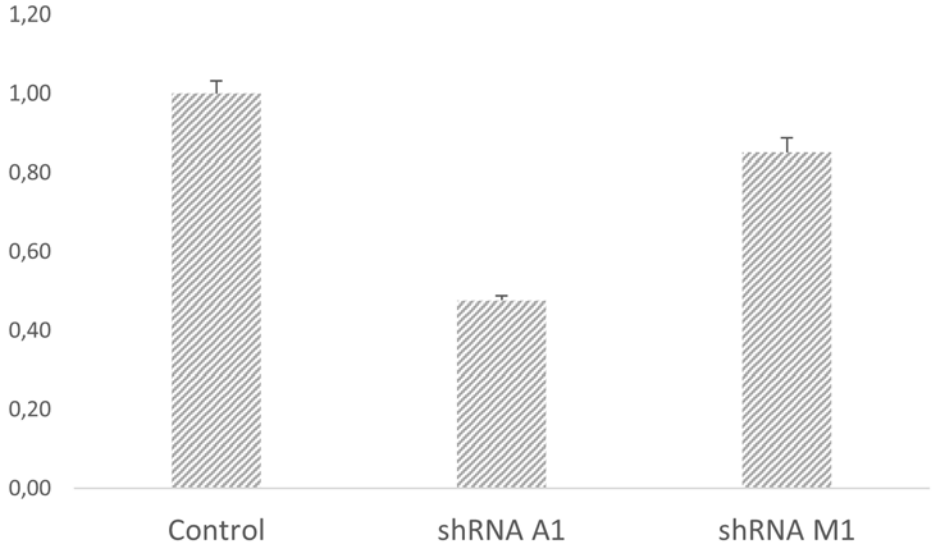

Figure S2. ***Acaca*** **knockdown transcript level analysis by Taqman qPC**R. Control: cells infected with virus carrying the empty RVH1 vector for control. shRNA A1: cells expressing an shRNA for KD of total Acaca transcript. Levels of mRNA were reduced by about 50%. sh RNA M1: KD construct targeting specifically the transcript encoding the putative MTS variant. Samples exhibited only a mild reduction of Acaca mRNA. Values are presented as group (n=3) means ± SD. The gene expression was normalized to 18S rRNA within each sample group; the value of the control esiRNA was designated as '1', and relative values are shown.

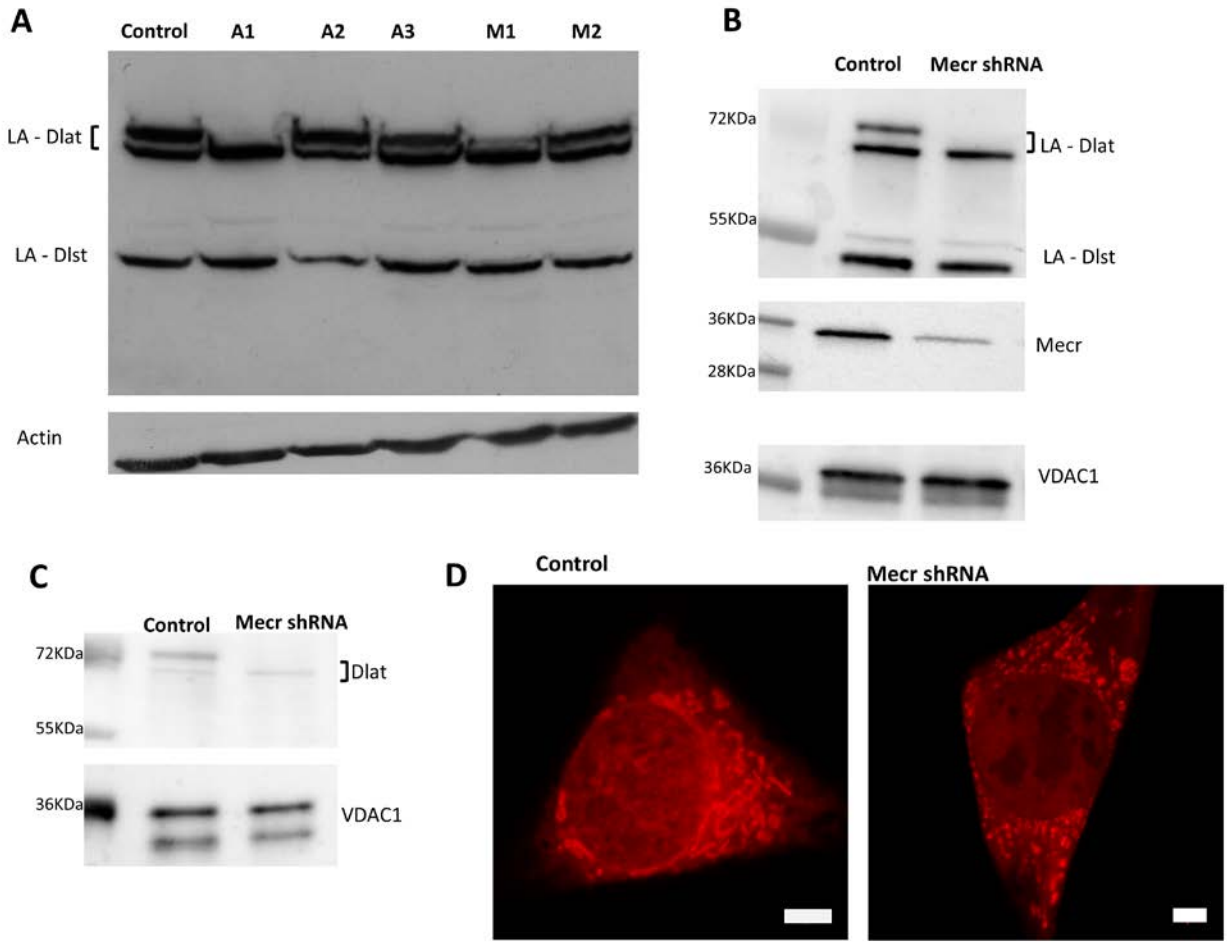

Figure S3. **Preliminary western blotting analysis of lipoylation in five Acaca KD candidates and effect of KD of *Mecr* encoding the 2-enoyl ACP reductase mtFAS component onprotein lipoylation and mitochondrial morphology in mouse cells. A**) Western analysis of whole cell extract five *Acaca* NIH3T3 candidate KD mouse cells lines initially showed separation of mouse lipoylated Dlat into two distinct bands, with loss of the upper LA-Dlat band in two successful KD candidates and no clear reduction of lipoylated Dlst (LA-Dlst) (loading control: anti-β actin). **B**) Western analysis mitochondrial extracts of NIH3T3 cells expressing *Mecr* shRNA, carried out with anti-Mecr (central panel), and the same anti-LA (Lipoic acid, upper panel) antiserum batch as in (**A**) also showed a specific loss of the upper LA-Dlat signal. **C**) Anti-Dlat (lower right panel) antibody was used to further confirm that the protein bands where lipoylation was affected were Dlat. Also in the Mecr KD cells, Dlat was lost concomitantly to lipoic acid loss. Anti-Porin

(VDAC1) antibody as a loading control. **D**) Fragmented mitochondrial morphology of NIH3T3 *Mecr* shRNA cells (right panel) compared to mostly reticular mitochondrial structure in control cells (left panel). Cells were visualized with MitoTracker Red CMXRos and the cells were imaged using confocal microscopy. Scale bars are 10 µm.

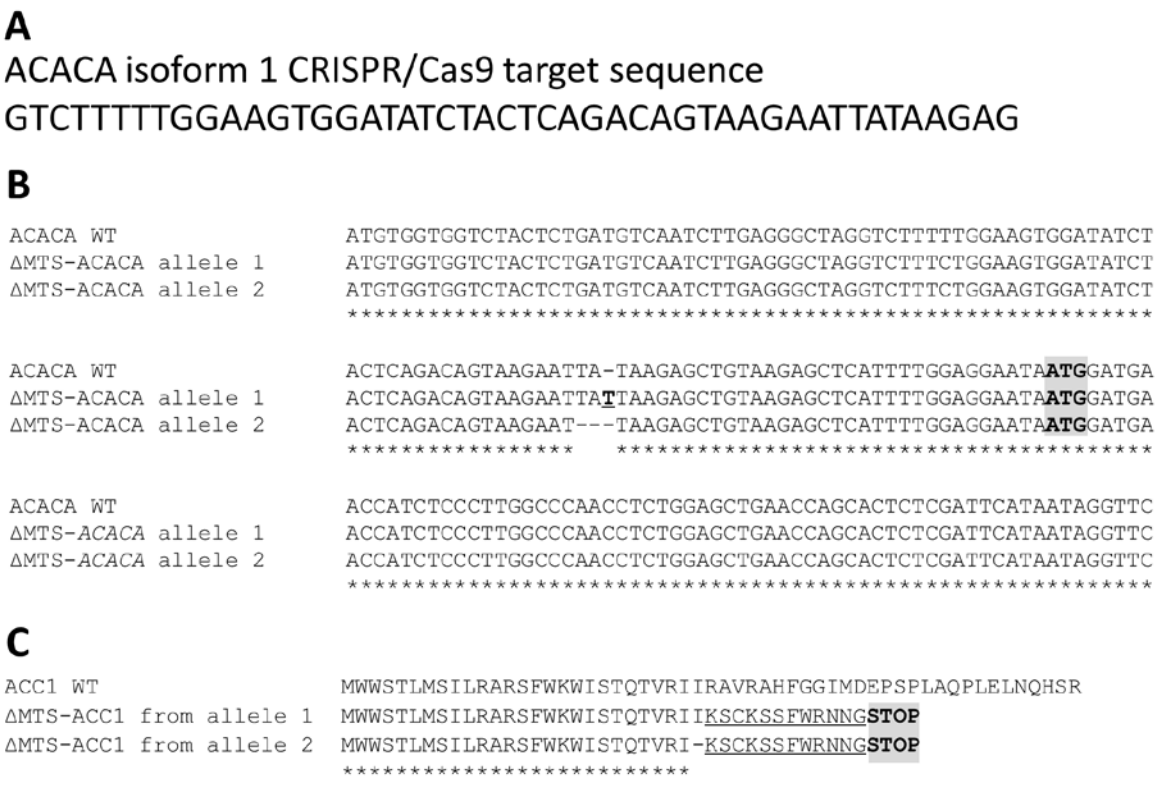

Figure S4. **CRISPR/Cas9 mediated genome editing of the sequence encoding the predicted MTS of human ACC1. A**) Target Sequence of the human ACACA gene (isoform 1) used for CRISPR/Cas9 editing. **B**) Editing both alleles in the ΔMTS-ACC1 cell line by CRISPR/Cas9 was confirmed by cloning and sequencing of both of the relevant ACACA regions. The sequence encoding the putative MTS was edited in both gene copies. Alignment of the DNA sequences DNA shows the insertion of one base pair in one allele and a 2 bp deletion in the other. The sequence following the start codon (marked in bold and by gray shading) for translation of cytosolic ACC1 is unaltered in the sequence, and the edited clone still produces full size ACC1 (Figure 4 in main text). **C**) Alignment of the N-terminal amino sequence of human wild type and ΔMTS-ACC1

showing the predicted amino acid sequence change (underlined) and location of the premature termination site (STOP, bold and in gray shading) resulting from the frameshift mutations in the ΔMTS-ACC1 edited cell line.

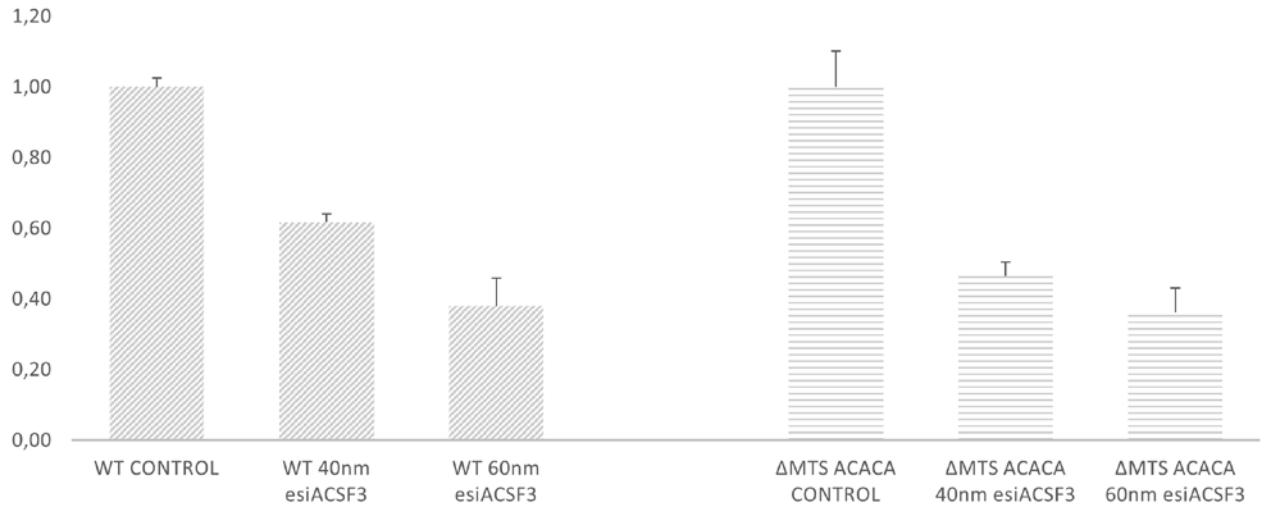

Figure S5. **Taqman qPCR analyses of ACSF3 expression levels after esiRNA treatment for WT and ΔMTS-ACACA cells**. Hela cells were transfected with esiRNA targeting ACSF3 at a final concentration of 40nM or 60nM. Left: transcription levels for the ACSF3 KD experiment in WT background. Right: transcription levels for the ACSF3 KD experiment in the background. Values are presented as group (n=4) means, Error bars indicate standard deviation. The gene expression was normalized to Actin B within each sample group; the value of the control esiRNA was designated as '1', and relative values are shown.

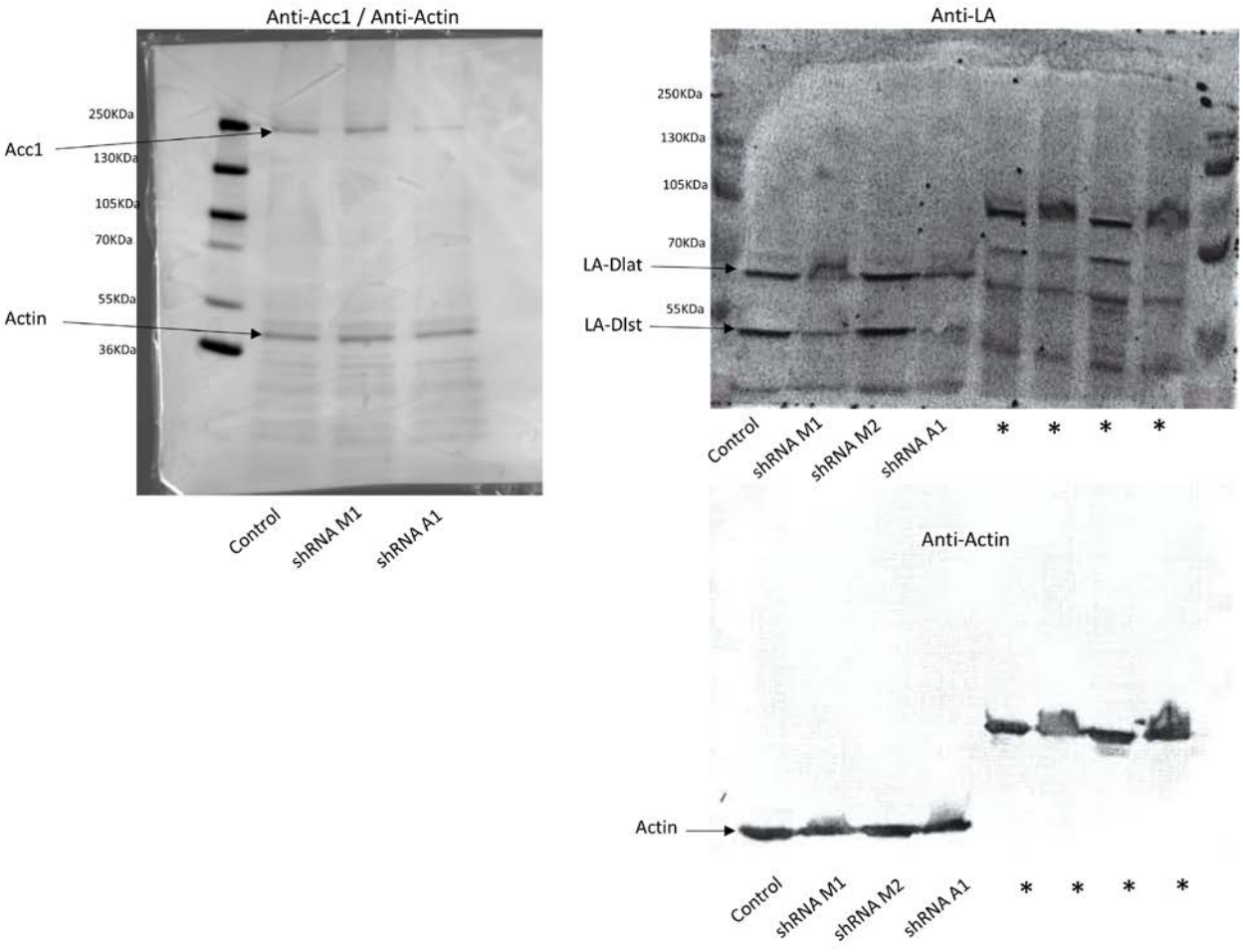

Figure S6. Complete western blots from Figure 2. * These lanes are not shown in the main manuscript file.

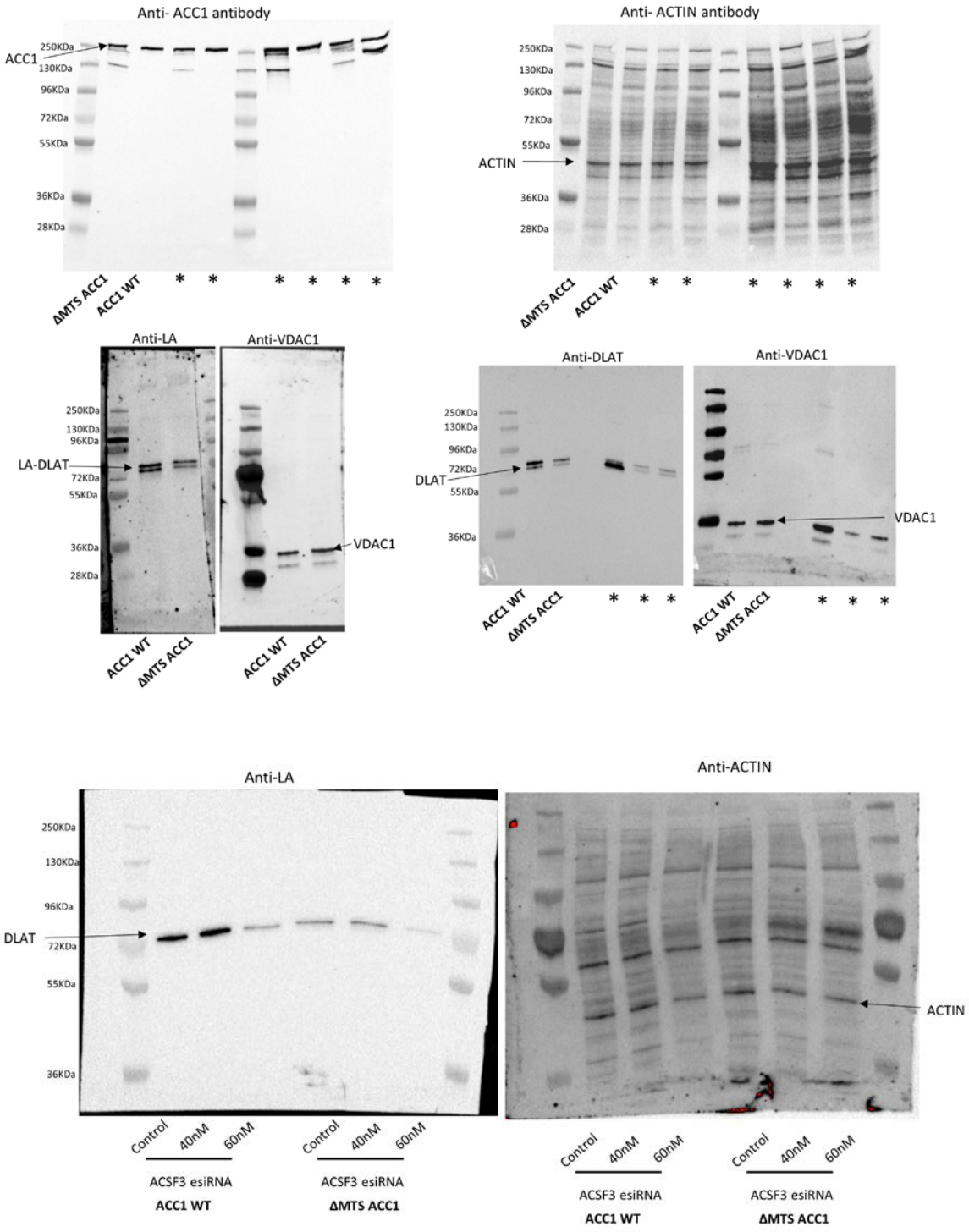

Figure S7: Complete western blots from Figure 3. * These lanes are not shown in the main manuscript file.

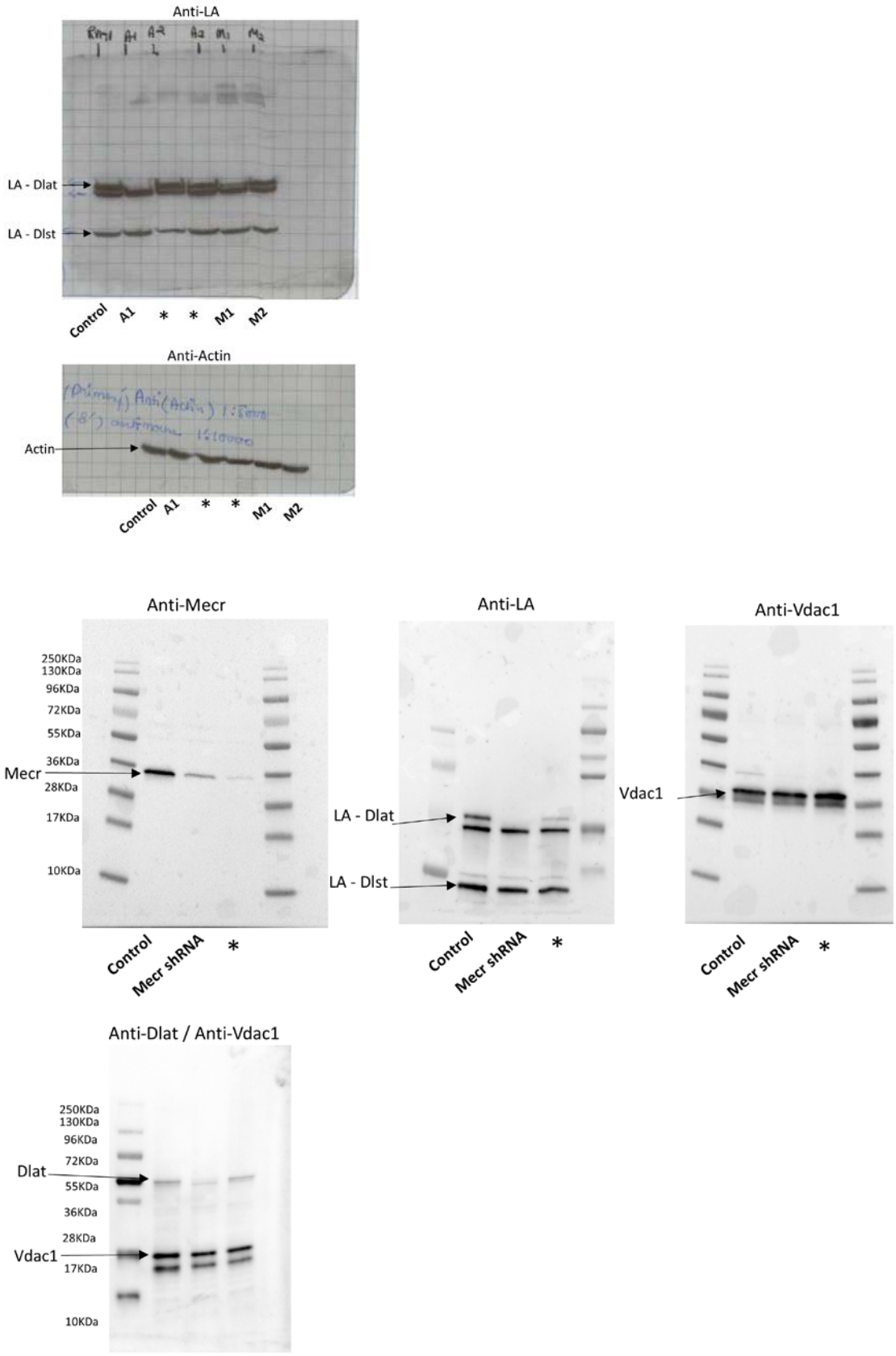

Figure S8: Complete western blots from Figure S3. * These lanes are not shown in the main manuscript file.

A conserved mammalian mitochondrial isoform of acetyl-CoA carboxylase ACC1 provides the malonyl-CoA essential for mitochondrial biogenesis in tandem with ACSF3

Geoffray Monteuuis, Fumi Suomia, Juha M. Kerätär, Ali J. Masud and Alexander J. Kastaniotis

Supplementary Experimental

Details: Generation of Acaca and Mecr shRNA Knockdowns. Acaca Knockdown. Detailed procedure. For infection with the KD constructs, cells were kept in high-glucose DMEM (4.5g/l) containing 10% FBS, and 2 mM L-glutamine. Nearly confluent cells in six-well plates were transfected with 4 μg of pRVH1-puro carrying the KD cassette and 0.4 μg of pVSV-G per well by using Fugene 6 (Promega, Madison, Wisconsin, USA) according to the manufacturer's protocol. Twenty-four hours post transfection, the medium was changed to low-glucose DMEM (1g/L) with the same supplements as above (1 ml per well), and placed at 37°C. Forty-eight hours post transfection, the medium was collected, and passed through a 0.45μm filter to clear off cell debris, and was used for the transduction of the NIH3T3 cells. The mouse 3T3 strain cells were cultured in DMEM with 10% FBS, 2 mM glutamine, and 100 units/ml penicillin and streptomycin. For infection, 300,000 cells were seeded in each well of a 6-well plate, and incubated at 37°C. After 24 hours, the medium was aspirated and 1ml of filtered supernatantvirus containing the virussupernatant, supplemented with 4 μg/ml polybrene (SIGMA-Aldrich Saint Louis, Missouri, USA) to a final concentration of 4 μg/ml were added. and 2 hours after exposure of the cells to adding the virus, 0.5 ml of OPTIMUM medium with 10% FBS was added. The infection was repeated 3 times. After 24 hours post-

transduction, the medium was changed to high-glucose DMEM (4.5 g/liter) containing 10% FBS and 2 mM L-glutamine and were returned to incubate at 37°C. After 72 hours post-infection, the cells were trypsinized and seeded into two six-well plates in the presence of 4 μg/ml puromycin (BD Biosciences). Selection was done for 5 days.

Details: Generation of HEK293 ΔMTS-ACC1 cell lines. HEK293T cells were transfected with the CRISPR/Cas9 genome editing construct custom designed and manufactured by SIGMA-Aldrich (SIGMA-Aldrich, Saint Louis, Missouri, USA) for the specified sequence. After 24h, cells were analyzed by fluorescence-activated cell sorting (FACS) to obtain cells that express green fluorescent protein (GFP). Growth of single cells in 96 well plates allowed the isolation of HEK293-derived cell clones that were candidates for the desired knockout cell line. Potential positive clones for ACACA MTS knockout (KO) were expanded and subjected to several assays to characterize the knockout cell lines. Heteroduplexes derived from PCR amplicons flanking the target site were subjected to T7E1 (T7 endonuclease I1, New England Biolabs, Ipswich, MA, USA) digests. The knockout cell line displayed heterozygosity at the target site, since cleaved DNA fragments were produced by T7E1 digestion. PCR products from WT HEK293 cells were mixed with PCR products from the mutant, re-annealed and treated with T7E1. The samples showed similar digestion patterns indicating that the clonal cell lines are heterozygous at the target sites.